

**Serotonin 5-HT_{1B} receptor-mediated calcium influx-independent presynaptic inhibition of
GABA release onto rat basal forebrain cholinergic neurons**

Takuma Nishijo & Toshihiko Momiyama*

Department of Pharmacology, Jikei University School of Medicine

Minato-ku, Tokyo 105-8461

Japan

Key words: slices, IPSCs, K⁺ channels, patch-clamp

***Correspondence should be addressed to: Toshihiko Momiyama, M.D., Ph.D.**

Department of Pharmacology, Jikei University School of Medicine

Nishi-Shimbashi, Minato-ku, Tokyo 105-8461

Japan

Phone: +81-3-3433-1111 ext. 2250

Fax: +81-3-5473-1428

E-mail: tmomi@jikei.ac.jp

Abstract

Modulatory roles of serotonin (5-HT) in GABAergic transmission onto basal forebrain cholinergic neurons were investigated, using whole-cell patch-clamp technique in the rat brain slices. GABA_A receptor-mediated inhibitory postsynaptic currents (IPSCs) were evoked by focal stimulation. Bath application of 5-HT (0.1-300 μ M) reversibly suppressed the amplitude of evoked IPSCs in a concentration-dependent manner. Application of a 5-HT_{1B} receptor agonist, CP93129, also suppressed the evoked IPSCs, whereas a 5-HT_{1A} receptor agonist, 8-OH-DPAT had little effect on the evoked IPSCs amplitude. In the presence of NAS-181, a 5-HT_{1B} receptor antagonist, 5-HT-induced suppression of evoked IPSCs was antagonized, whereas NAN-190, a 5-HT_{1A} receptor antagonist did not antagonize the 5-HT-induced suppression of evoked IPSCs. Bath application of 5-HT reduced the frequency of spontaneous miniature IPSCs without changing their amplitude distribution. The effect of 5-HT on miniature IPSCs remained unchanged when extracellular Ca²⁺ was replaced by Mg²⁺. The paired-pulse ratio was increased by CP93129. In the presence of ω -CgTX, the N-type Ca²⁺ channel blocker, ω -Aga-TK, the P/Q-type Ca²⁺ channel blocker, or SNX-482, the R-type Ca²⁺ channel blocker, 5-HT could still inhibit the evoked IPSCs. 4-AP, a K⁺ channel blocker, enhanced the evoked IPSCs, and CP93129 had no longer inhibitory effect in the presence of 4-AP. CP93129 increased the number of action potentials elicited by depolarizing current pulses. These results suggest that activation of presynaptic 5-HT_{1B} receptors on the terminals of GABAergic afferents to basal forebrain cholinergic

neurons inhibits GABA release in Ca^{2+} influx-independent manner by modulation of K^+ channels, leading to enhancement of neuronal activities.

Abbreviations

BF, basal forebrain; CNQX, 6-Cyano-7-nitroquinoxaline-2,3-dione; CP93129, 1,4-Dihydro-3-(1,2,3,6-tetrahydro-4-pyridinyl)-5*H*-pyrrol[3,2-*b*]pyridin-5-one dihydrochloride; D-AP5, D-(-)-2-amino-5-phosphonopentanoic acid; 8-OH-DPAT, (R)-(+)-8-Hydroxy-DPAT hydrobromide; GABA, γ -aminobutyric acid; 5-HT, serotonin; IPSCs, inhibitory postsynaptic currents; eIPSCs, evoked IPSCs; mIPSCs, miniature IPSCs; NAN-190, 1-(2-Methoxyphenyl)-4-(4-phthalimidobutyl)piperazine hydrobromide; NAS-181, (2*R*)-2-[[[3-(4-Morpholinylmethyl)-2*H*-1-benzopyran-8-yl]oxy]methyl]morpholine dimethanesulfonate; TTX, tetrodotoxin; ω -GgTX, ω -conotoxin GVIA; ω -Aga-TK, ω -agatoxin TK; 4-AP, 4-aminopyridine.

Introduction

Serotonin (5-HT) is a neuromodulator originating in the dorsal raphe nuclei (DRN) (Daubert & Condron, 2010). It has been suggested that central 5-HT systems are involved in anxiety-like behaviours, disorder of which could lead to depression (Ressler & Nemeroff, 2000; Lowry *et al.*, 2005). Actually 5-HT-related drugs, especially selective serotonin uptake inhibitors (SSRIs), are clinically used for ameliorating the symptoms in such disorders (Bandelow *et al.*, 2008). However, the mechanisms underlying the overall roles of central 5-HT systems as well as the action of medications for the treatment of anxiety disorders are still ambiguous, probably due to the diversity of central 5-HT receptors (Pytliak *et al.*, 2011). Therefore, analyses in the levels of cellular neurophysiology regarding the roles of 5-HT receptor subtypes are essential for the better understandings of central 5-HT systems in the control of mood or anxiety behaviours.

Serotonergic fibres project and innervate various brain areas including basal forebrain (BF) nuclei (Gasbarri *et al.*, 1999; Sari *et al.*, 1999). BF is an origin of cholinergic neurons which project to various brain regions containing cortex and hippocampus (Rye *et al.*, 1984), and has been shown to be involved in attention, arousal, learning, memory and sleep-wake states, as well as the related disorder, including dementia and Alzheimer's disease (Coyle *et al.*, 1983; Oyanagi *et al.*, 1989; Zant *et al.*, 2016). Therefore, BF-related physiological functions as well as their disorders could be affected by 5-HT system. Previous morphological studies have shown that cholinergic neurons in the BF receive abundant inhibitory GABAergic synaptic inputs mainly from the nucleus accumbens (Zaborszky *et al.*,

1986; Heimer *et al.*, 1991; Zaborszky & Culliman, 1992; Chang *et al.*, 1995) as well as from GABAergic neurons within the BF (Sun & Cassell, 1993). It has been reported that GABAergic inhibitory postsynaptic currents (IPSCs) recorded in putative cholinergic neurons in the BF were inhibited by activation presynaptically located dopamine D₁-like receptors (Momiya & Sim, 1996). However, 5-HT-induced modulatory effects on the synaptic transmission in the BF are unknown. Therefore, this study was aimed to elucidate 5-HT-induced modulation of GABAergic synaptic transmission onto cholinergic neurons in the BF. The present results have demonstrated that 5-HT acts on 5-HT_{1B} receptors located on the GABAergic presynaptic terminals, thereby inhibiting GABA release onto cholinergic neurons, and that the inhibition is independent of Ca²⁺ influx into the GABAergic terminals.

Methods

Injection of Cy3-192IgG

All experimental procedures were approved by the Animal Care and Use Committee of the Jikei University School of Medicine. In this study, 77 young Slc:SD rats (8-12 days old, supplied by Japan SLC Inc.) were used. Rats were anaesthetized with pentobarbital (50 mg/kg i.p.) and then mounted into a stereotaxic apparatus (Narishige, Tokyo, Japan). Cy3-192IgG (3 µl; 0.7mg/ml) was injected unilaterally into the lateral ventricle of the rat using a Hamilton syringe (22 gauge needle) at a rate of 0.5 µl/min (Wu *et al.*, 2000; Momiya & Zaborszky, 2006; Momiya & Fukazawa, 2007). The

coordinates of the lateral ventricle used were 1.0 mm posterior from Bregma, 1.0 mm lateral from midline, and 4.0 mm below from the dura.

Slice preparation

Three to seven days following intracerebroventricular injection of Cy3-192IgG, rats (postnatal days 12-19) were killed by decapitation under deep halothane or isoflurane anaesthesia, according to the guidance of the Animal Care and Use Committee of the Jikei University School of Medicine, mainly to avoid liver toxicity of humans, and coronal slices containing the basal forebrain regions including the substantia innominata (SI) and the horizontal limb of the diagonal band of Broca (HDBB), were cut (300 μm thick) using microslicer (PRO7, Dosaka, Kyoto, Japan) in ice-cold oxygenated cutting Krebs solution of the following composition (mM): choline chloride, 120; KCl, 2.5; NaHCO₃, 26; NaH₂PO₄, 1.25; D-glucose, 15; ascorbic acid, 1.3; CaCl₂, 0.5; MgCl₂, 7. The slices were then transferred to a holding chamber containing standard Krebs solution of the following composition (mM): NaCl, 124; KCl, 3; NaHCO₃, 26; NaH₂PO₄, 1; CaCl₂, 2.4; MgCl₂, 1.2; D-glucose, 10; pH 7.4 when bubbled with 95% O₂-5% CO₂. Slices were incubated in the holding chamber at room temperature (21-26°C) for at least 1 hour before recording.

Whole-cell recording and data analysis

For recoding, a slice was transferred to the recoding chamber, held submerged, and superfused with standard Krebs solution (bubbled with 95% O₂-5% CO₂) at a rate of 3-4 ml/min. Neurons in the SI or HDBB were visually identified with a 60 x water immersion objective attached to an upright microscope (BX50WI, Olympus Optics, Tokyo, Japan). Images were detected with a cooled CCD camera (CCD-300T-RC, Nippon roper, Tokyo, Japan) and displayed on a video monitor (LC-150M1, Sharp, Osaka, Japan). Cy3-192IgG-labelled neurons were visualized using the appropriate fluorescence filter (U-MWIG3, Olympus Optics, Tokyo, Japan). Patch pipettes for whole-cell recording were made from standard-walled borosilicate glass capillaries (1.5 mm outer diameter; Harvard Apparatus, Kent, UK). For the recording of evoked or miniature synaptic currents, patch pipettes were filled with a cesium chloride-based internal solution of the following composition (mM): CsCl, 140; NaCl, 9; Cs-EGTA, 1; Cs-HEPES, 10; Mg-ATP, 2 (pH adjusted with 1 M CsOH). For current-clamp recordings, patch pipettes were filled with a potassium gluconate-based internal solution of the following composition (mM): potassium gluconate, 120; NaCl, 6; CaCl₂, 5; MgCl₂, 2; K-EGTA, 0.2; K-HEPES, 10; Mg-ATP, 2; Na-GTP, 0.3 (pH adjusted with 1 M KOH). Whole-cell recordings were made from Cy3-192IgG-labelled neurons using a patch-clamp amplifier (Axopatch 200B, Molecular Devices, Foster City, CA, USA). The cell capacitance and the series resistance were measured from the amplifier. The access resistance was monitored by measuring capacitive transients obtained in response to a hyperpolarizing voltage step (5 mV, 25 ms) from a holding potential of -65 mV. Only data recorded with access resistance < 20 MΩ were used for the analysis. No correction was made for

the liquid junction potentials (calculated to be 5.0 mV by pCLAMP7 software, Molecular Devices). Synaptic currents were evoked via an external stimulating electrode filled with 1 M NaCl, using voltage pulses (0.2-0.4 ms in duration) of suprathreshold intensity at a rate of 0.2 Hz (every 5 s). Paired-pulse stimuli were applied with an interstimulus interval of 50 ms (Momiya & Fukazawa, 2007). The stimulating electrode was placed within 50-120 μm radius of the recorded neuron. The position of the stimulating electrode was varied until a stable response was evoked in the recorded neuron. All the inhibitory postsynaptic currents (IPSCs) were evoked at a holding potential of -65 mV. Experiments were carried out at room temperature (21-26°C).

Data were stored on digital audio tapes using a DAT recorder (DC to 10 kHz; Sony, Tokyo, Japan). Evoked IPSCs were digitized off-line at 10 kHz (low-pass filtered at 2 kHz with an 8-pole Bessel filter) using pCLAMP9 software (Molecular Devices). The effects of drugs on the evoked IPSCs were assessed by averaging their amplitudes for 100 s (20 traces) after the effect had reached the steady state and comparing this value with the averaged amplitude of 20 traces just before the drug application. Miniature IPSCs (mIPSCs) were filtered at 2 kHz and digitized at 20 kHz using pCLAMP9 software and analyzed using N software (provided by Dr. S. F. Traynelis, Emory University). The effect of 5-HT on mIPSCs was assessed by comparing the frequency and amplitude distribution of the events for 3 min during the peak response to 5-HT with those obtained just before 5-HT application. The concentration-response curve was fitted to the theoretical equation:

$$Y = A \left(1 - \frac{1}{1 + (X/X_0)^n} \right)$$

where Y is the percentage inhibition of IPSCs, X is the concentration of 5-HT, A is the maximal percentage inhibition of IPSCs, X_0 is the IC_{50} , and n is the Hill slope. The fitting was done using the embedded logistic function in ORIGIN (Microcal Software, Northampton, MA, USA). An apparent dissociation constant (K_B) for NAS-181, a 5-HT_{1B} receptor antagonist, was calculated using the equation:

$$K_B = [B]/(DR - 1),$$

where $[B]$ is the concentration of NAS-181 and DR (dose ratio) is the ratio of IC_{50} values for pooled data observed in the presence and absence of the antagonist, assuming that NAS-181 behaves as a competitive antagonist. Statistical analysis was carried out using both Student's t test (two-tailed) and a non-parametric Mann-Whitney U test. The Kolmogorov-Smirnov (K-S) test was used for the comparison of cumulative probability distribution of mIPSCs. In all statistics, a P value of 0.05 was used as the confidence limit and data are expressed as means \pm SEM.

Drugs

Cy3-192IgG was custom-synthesized by Advanced Targeting Systems (San Diego, CA, USA). Synthetic ω -conotoxin GVIA (ω -GgTX), ω -agatoxin TK (ω -Aga-TK) and SNX-482 were purchased from Alamone Labs (Jerusalem, Israel). These toxins were dissolved in oxygenated perfusing solution containing cytochrome c (1 mg/ml, Sigma). Other drugs were stored as frozen stock solutions and dissolved in the perfusing solution just before application in the final concentration indicated. 6-

Cyano-7-nitroquinoxaline-2,3-dione (CNQX), D-(-)-2-amino-5-phosphonopentanoic acid (D-AP5), bicuculline methochloride, 1,4-Dihydro-3-(1,2,3,6-tetrahydro-4-pyridinyl)-5H-pyrrol[3,2-b]pyridin-5-one dihydrochloride (CP93129), (2R)-2-[[[3-(4-morpholinylmethyl)-2H-1-benzopyran-8-yl]oxy]methyl]morpholine dimethanesulfonate (NAS-181) and 1-(2-Methoxyphenyl)-4-(4-phthalimidobutyl)piperazine hydrobromide (NAN-190) were from Tocris Bioscience (Bristol, UK). Strychnine, serotonin hydrochloride and (R)-(+)-8-Hydroxy-DPAT hydrobromide (8-OH-DPAT) were from Sigma (St. Louis, MO, USA). Tetrodotoxin (TTX) and 4-aminopyridine (4-AP) were from Sankyo (Tokyo, Japan). All drugs were bath applied.

Results

Identification of cholinergic neurons in the basal forebrain

Whole-cell recordings were made from a total of 177 Cy3-192IgG-stained neurons within the BF region. Figure 1A shows BF neurons lying within a slice under infrared-differential interference contrast (IR-DIC) microscopy and Fig. 1B under fluorescence optics to reveal staining with Cy3-192IgG. Synaptic currents were evoked at a rate of 0.2 Hz (every 5 s) at a holding potential of -65 mV by focal stimulation in the presence of CNQX (5 μ M), strychnine (0.5 μ M) and D-AP5 (25 μ M) to block non-NMDA glutamatergic, glycinergic and NMDA glutamatergic components, respectively.

These synaptic currents were reversibly blocked by bath application of bicuculline (10 μM) in all 5 neurons tested (Fig. 1, C1 and C2), revealing that they were GABAergic in nature.

Effect of 5-HT on the evoked IPSCs

Bath application of 5-HT (1 μM) gradually inhibited the amplitude of the evoked IPSCs (eIPSCs), and the effect reached its steady state in several minutes (Fig. 2A). The eIPSCs recovered after 5-10 minutes of washout (Fig. 2A). The 5-HT-induced inhibitory effect on the eIPSCs was concentration dependent between 0.1 and 300 μM . Figure 2B shows the concentration-response curve of the 5-HT effect, giving an apparent IC_{50} value, maximum eIPSC depression and Hill slope value of 1.89 μM , 65.0% and 1.04, respectively. Concentration of 5-HT used in this study had little or no direct effect on the holding currents at -65 mV with CsCl-based GTP-free internal solution.

Pharmacological identification of 5-HT receptor subtypes

To identify the subtypes of 5-HT receptor involved in inhibitory effect, the effects of 5-HT receptor agonist (Fig. 3) and antagonists (Fig. 4) were examined.

Effect of 5-HT receptor agonists on the evoked IPSCs

First, the effects of a selective 5-HT_{1A} receptor agonist, 8-OH-DPAT, 10 μM , and a selective 5-HT_{1B} receptor agonist, CP93129 (1 and 10 μM), on the amplitude of eIPSCs were compared with those of

5-HT (Fig. 3). 8-OH-DPAT had little or no effect on the amplitude of eIPSCs (Fig. 3A), with an apparent inhibition of eIPSCs by $11.2 \pm 6.12\%$ ($n = 6$, Fig. 3C). On the other hand, CP93129 at concentrations 1 and $10\mu\text{M}$ inhibited the amplitude of eIPSCs by $67.6 \pm 7.13\%$ ($n = 5$) and $52.5 \pm 5.50\%$ ($n = 11$) respectively (Fig. 3B and C). As shown in Figure 3C, CP93129-induced inhibitory effect was not significantly ($P = 0.349$) different from that of 5-HT at the corresponding concentrations, whereas 8-OH-DPAT-induced inhibition was significantly ($P = 0.0003$) smaller than that of 5-HT. These findings imply that the action of 5-HT is mediated by 5-HT_{1B} receptors.

Effect of 5-HT receptor antagonists on the 5-HT-induced inhibition of evoked IPSCs

To determine that 5-HT-induced inhibition in BF cholinergic neurons is mediated by 5-HT_{1B} receptors, we examined the effect of a 5-HT_{1A} receptor antagonist, NAN-190 ($30\mu\text{M}$), and 5-HT_{1B} receptor antagonist, NAS-181 ($30\mu\text{M}$), on the 5-HT-induced inhibition of eIPSCs. Bath application of $30\mu\text{M}$ NAN-190 or NAS-181 had no effect of the eIPSCs. After confirming the effect of 5-HT and recovery following washout, the antagonist was applied for at least 5 minutes, before 5-HT was applied again in the presence of the antagonist. As expected, NAS-181 antagonized the 5-HT ($10\mu\text{M}$)-induced inhibitory effect on the eIPSCs (Fig. 4A), whereas NAN-190 did not antagonize the 5-HT-induced inhibition of eIPSCs (Fig. 4B).

The concentration-response curve for 5-HT was shifted to the right in the presence of NAS-181, with an IC₅₀ value, maximum eIPSC depression and Hill slope value was $33.4\mu\text{M}$, 61.6% and 2.31,

respectively (Fig. 4C). From this shift, an apparent K_B value for NAS-181 was calculated to be 0.70 μM (pK_B 6.2). On the other hand, 5-HT (10 μM)-induced inhibition of eIPSCs in the presence of NAN-190 was $65.0 \pm 5.80\%$ ($n = 6$), which was not significantly ($P = 0.484$) different from that by 5-HT alone in the corresponding neurones ($59.4 \pm 5.10\%$, $n = 6$), supporting the lack of involvement of 5-HT_{1A} receptors.

Effect of 5-HT on miniature IPSCs

To ascertain whether the modulatory effect of 5-HT on GABAergic transmission was presynaptic or postsynaptic, we examined the effect of 5-HT on miniature IPSCs (mIPSCs). The mIPSCs were recorded in the presence of tetrodotoxin (TTX, 0.5 μM) in addition to CNQX (5 μM), strychnine (0.5 μM) and D-AP5 (25 μM). The frequency of mIPSCs was 0.82 ± 0.18 Hz ($n = 6$) in normal 2.4 mM external Ca^{2+} concentration. Bath application of 5-HT (1 μM) reduced the frequency of mIPSCs and the effect reached its steady state in 3 minutes (Fig. 5A). Figure 5B and C illustrate the cumulative probability distributions for the effect of 5-HT on mIPSC inter-event interval and amplitude respectively. 5-HT reduced the frequency of mIPSCs and significantly shifted the inter-event intervals ($P = 0.00000006$, K-S test) (Fig. 5B), whereas the amplitude of mIPSCs was not significantly affected by 5-HT ($P = 0.380$, K-S test) (Fig 5C and D). 5-HT inhibited the frequency of mIPSCs by $52.9 \pm 11.6\%$ ($n = 6$) (Fig. 5E) but had no effect on the mean amplitude of mIPSCs ($1.27 \pm 11.9\%$, $n = 6$).

These results indicate that 5-HT acts on presynaptic terminals and inhibits GABA release without affecting postsynaptic GABA_A receptor sensitivity.

To assess whether the inhibitory effect of 5-HT on presynaptic terminals is targeted to Ca²⁺ entry or the release machinery itself, we examined the effect of 5-HT in Ca²⁺-free, 5 mM Mg²⁺ external solution. The frequency of mIPSCs was 0.52 ± 0.16 Hz (n = 6) in Ca²⁺-free external solution. 5-HT inhibited the frequency of mIPSCs by $41.1 \pm 10.4\%$ (n = 6) in Ca²⁺-free external solution and this effect was not significantly ($P = 0.463$) different from that in normal Ca²⁺ (2.4 mM) external solution (Fig. 5E). The amplitude of mIPSCs was not significantly affected by 5-HT in Ca²⁺-free external solution. These results suggest that 5-HT does not affect Ca²⁺ entry but the release machinery itself, and reduced GABA release.

Effects of CP93129 on paired-pulse ratio

To further confirm the presynaptic site of action, the effects of CP93129 on paired-pulse ratio were examined. In the GABAergic synapse onto BF cholinergic neurons, paired-pulse facilitation or paired-pulse depression was observed with an interstimulus interval of 50 ms depending on the cells. The ratio (IPSC₂/IPSC₁, where IPSC₁ and IPSC₂ correspond to the peak amplitude of the first and second IPSCs, respectively) was 0.75 ± 0.05 (n = 8) in the normal external solution. The ratio was increased to 1.16 ± 0.12 (n = 8) by application of CP93129 (Fig. 6A and B), that was significantly ($P = 0.007$)

larger than that of control. These results further suggest the presynaptic locus of 5-HT_{1B} receptor-mediated inhibition of GABA release onto BF cholinergic neurons.

Ca²⁺ channel subtype contributing to eIPSCs

The above findings that 5-HT had no effect on mIPSCs in the nominally Ca²⁺-free solution indicate that 5-HT does not affect Ca²⁺ entry. To further examine this issue, experiments were carried out using selective blockers for Ca²⁺ channel subtypes. To identify Ca²⁺ channel subtypes involved in eIPSCs, we examined the effect of ω -conotoxin (ω -CgTX), an N-type Ca²⁺ channel blocker, ω -agatoxin-TK (ω -Aga), a P/Q-type Ca²⁺ channel blocker, and SNX-482, an R-type Ca²⁺ channel blocker. Bath application of ω -CgTX (3 μ M) gradually inhibited the amplitude of the eIPSCs, and the effect reached a steady state after several minutes (Fig. 7A). Additional bath application of ω -Agatoxin-TK (200 nM) largely inhibited the remaining fraction of the IPSCs (Fig. 7A). A similar consequence was found when ω -Agatoxin-TK (200 nM) was applied first, followed by additional application of ω -CgTX (3 μ M) (Fig. 7B), with resultant inhibition of eIPSCs by ω -CgTX (3 μ M), ω -Aga (200 nM) and both toxins being $60.1 \pm 4.85\%$ (n = 9), $47.4 \pm 7.52\%$ (n = 10) and $89.7 \pm 3.66\%$ (n = 6) respectively (Fig. 7C). However, SNX-482 had little effect on the amplitude of eIPSCs with an apparent inhibition of $7.41 \pm 5.07\%$ (n = 13) (Fig. 7C). Assuming a power function for the relationship between presynaptic Ca²⁺ concentration and transmitter release, the relative amplitude of postsynaptic currents remaining after application of ω -CgTX (A), ω -Agatoxin-TK (B) or both toxins (C) can be described as $A = (1 - a)^m$, B

$= (1 - b)^m$ and $C = c^m$, where a , b and c represent a fraction of presynaptic Ca^{2+} channel subtypes sensitive to ω -CgTX (a), ω -Agatoxin-TK (b) and those insensitive to these toxins (c), and m is the power coefficient (Takahashi & Momiyama, 1993; Momiyama & Koga, 2001). If each toxin at the present concentration selectively blocks only one presynaptic Ca^{2+} channel subtype, $a + b + c$ should be unity. Previous studies have shown that the power coefficient is around 3 (Dodge & Rahamimoff, 1967; Augustine & Charlton, 1986; Takahashi, 1992; Takahashi & Momiyama, 1993; Momiyama & Koga, 2001). Assuming $m = 3$, the value was 0.923 ($a = 0.258$, $b = 0.195$, $c = 0.470$), showing that the value 'c' as apparently larger than 'a' or 'b', and the total value is considerably less than 1. If m is assumed to be 1.64, $a + b + c$ is 1.00 ($a = 0.422$, $b = 0.328$, $c = 0.250$), suggesting the plausible power function.

Ca²⁺ channel subtype involved in the inhibitory effect of 5-HT

To examine whether Ca^{2+} channels are involved in the modulatory role of 5-HT on GABAergic transmission, we tested the inhibitory effect of 5-HT in the presence of Ca^{2+} channel blockers. After the recovery of eIPSC amplitude from 5-HT (10 μM)-induced inhibition, one of the Ca^{2+} channel blockers was applied, and when the inhibition had reached a steady state, 5-HT (10 μM) was applied again in the presence of the blocker. In the presence of ω -CgTX (3 μM), 5-HT inhibited eIPSCs by $53.0 \pm 6.92\%$ ($n = 6$, Fig. 8A) and the inhibition was not significantly different from inhibition of eIPSCs by 5-HT in the absence of ω -CgTX ($61.8 \pm 6.99\%$, $n = 6$, $P = 0.373$, Fig. 8C). In the presence of ω -Aga-TK (200 nM, Fig. 8B) or in the presence of SNX-482 (300 nM), 5-HT also

inhibited IPSCs by $62.8 \pm 11.1\%$ and $68.5 \pm 6.12\%$, respectively. These were not significantly different from inhibition of IPSCs by 5-HT in the absence of ω -Aga-TK ($57.3 \pm 4.98\%$, $n = 7$, $P = 0.524$, Fig. 8C) or SNX-482 ($58.8 \pm 5.25\%$, $n = 5$, $P = 0.254$, Fig. 8C) respectively.

Involvement of K⁺ channels in 5-HT_{1B} receptor-mediated inhibition

The present results with Ca²⁺ channel blockers suggest that 5-HT inhibits GABA release independently to Ca²⁺ influx to presynaptic terminals. Therefore, as one of other ionic mechanisms, the involvement of presynaptic K⁺ channels was examined using 4-AP, a blocker of broad spectrums of K⁺ channels (Ishikawa *et al.*, 2003). After the recovery of the IPSC amplitude from CP93129 (10 μ M)-induced inhibition, 4-AP at a concentration of 100 μ M was applied to the bath. Similar to the previous report (Ishikawa *et al.*, 2003), bath application of 4-AP (100 μ M) increased the IPSC amplitude more than 2 folds (Fig. 9A and B, increased to $212.1 \pm 50.5\%$, of the value before 4-AP application, $n = 6$).

The time course plot in Figure 9A as well as Figure 3B shows that the IPSC amplitude did not fully recover from CP93129-induced inhibition despite the prolonged wash-out, suggesting that full recovery is not always possible because of many complicating factors including deteriorating cell conditions. As 4-AP may still have strong effect even when cells are not in good condition and other drugs such as CP93129 are no longer effective, the possibility could not be excluded that the lack of second application of CP93129-induced effect was due to a deteriorated cell condition. Therefore, 4-

AP was applied without first application of CP93129. In this condition, 4-AP (100 μ M) increased the IPSC amplitude to $204.3 \pm 31.7\%$ of the value before 4-AP application (Fig. 9B, $n = 6$), that was not significantly ($P = 0.901$) different from the enhancement when 4-AP was applied after first application of CP93129 ($212.1 \pm 50.5\%$, of the value before 4-AP application, $n = 6$). Therefore, data in these 12 neurons were pooled. After the 4-AP-induced effect had reached a steady state, CP93129 (10 μ M) was applied again in the presence of 4-AP. In the presence of 4-AP, CP93129 (10 μ M)-induced effect was $8.51 \pm 2.87\%$ ($n = 12$), significantly ($P = 0.0005$) smaller than the value with CP93129 without 4-AP ($46.3 \pm 6.10\%$, $n = 6$). These results suggest that the lack of CP93129-induced effect was not due to a deteriorated cell condition, confirming the involvement of 4-AP-sensitive K^+ channels in 5-HT_{1B} receptor mediated inhibition.

Effect of CP93129 on firings of BF cholinergic neurons

Finally, effect of activation of 5-HT_{1B} receptors on the firing of BF cholinergic neurons was examined. Under the present whole-cell current-clamp recordings using K-gluconate-based internal solution, the resting membrane potential of BF cholinergic neurons was -58.1 ± 2.12 mV ($n = 20$), and the neurons did not fire action potentials spontaneously. Therefore, effect of CP93129 (10 μ M) on the depolarizing pulse-induced firing was tested (Fig. 10A). In 19 neurons tested, the number of action potentials increased in 12 neurons, decreased in 2 neurons, in the remaining 5 neurons the number unchanged (Fig. 10B). Pooled data show that the number of action potentials elicited by a

depolarizing pulse current in control condition was 4.74 ± 0.62 (n = 19), that was increased to 5.42 ± 0.62 (n = 19) in the presence of CP93129 by the same depolarizing current pulse (Fig. 10B). CP93129-induced increase in the number of action potentials was significant ($P = 0.006$, paired t -test). On the other hand, CP93129 had no effect on the resting membrane potential of the tested neurons.

As shown in Figure 10A, in 10 out of 19 neurons examined in current-clamp recordings, outward synaptic potentials were observed on the membrane potentials by application of current steps (Fig. 10A). These potentials were almost insensitive to CNQX (5 μ M), but were blocked by bicuculline (10 μ M) in all of 8 neurons examined (data not shown), suggesting that most of the detected synaptic potential were GABA_A receptor-mediated inhibitory postsynaptic potentials (IPSPs). It is likely that excitatory postsynaptic potentials could not be detected in the experimental condition, probably due to lower signal to noise ratio. The IPSPs were not consistently affected by CP93129 (10 μ M), unlike pharmacologically isolated IPSCs clamped at -65 mV. Although these synaptic potentials may affect the triggering of the action potentials, detailed modulatory roles of 5-HT_{1B} receptors *in vivo* remains to be elucidated in future studies.

Discussion

This study has shown that activation of presynaptically-located serotonin 5-HT_{1B} receptors inhibits GABA release onto cholinergic neurons in the rat basal forebrain. The present data have also shown

that the presynaptic inhibition is not sensitive to Ca^{2+} channel blockers, and that the inhibition is mediated by 4-AP-sensitive K^+ channel modulation. As 4-AP could also have postsynaptic effects on 5-HT_{1B} receptor mediated response, contribution of postsynaptic mechanisms could not be excluded in the modulation of neuronal activities.

Presynaptic inhibition by 5-HT_{1B} receptors

In the present pharmacological assay, both the agonist and antagonist selective for 5-HT_{1A} receptors were without effects, at concentrations that were clearly effective at other central synapses (Koyama *et al.*, 1999). In contrast, a 5-HT_{1B} receptor selective antagonist, NAS-181, antagonized the 5-HT-induced suppression of eIPSCs. In fact, the presence of 5-HT_{1B} receptors have been reported in BF (Sari *et al.*, 1999). The affinity of a reversible competitive antagonist (K_B) is independent of the relationship between the response and the receptor occupancy by the agonist, thus crucial for identifying the receptor type involved. The estimates of the present K_B value for NAS-181 was 0.70 μM ($\text{p}K_B$ 6.2), which was similar to that for the other 5-HT_{1B} selective antagonists (Hannon & Hoyer, 2008). These results suggest that the 5-HT-induced inhibition observed in this study is likely to be mediated by 5-HT_{1B} receptors.

In this study, 5-HT reduced the frequency of mIPSCs without affecting their mean amplitude. Furthermore, paired-pulse ratio was increased by a 5-HT_{1B} receptor agonist. These findings as well as the lack of CP93129-induced effect on the resting membrane potential or the holding current suggest

the presynaptic locus of 5-HT_{1B} receptor-mediated inhibition. 5-HT-induced presynaptic inhibitory effects have been reported in several central synapses (Umemiya & Berger, 1995; Hori *et al.*, 1996; Koyama *et al.*, 1999; Blackmer *et al.*, 2001; Mizutani *et al.*, 2006; Fukushima *et al.*, 2009; Guo & Rainnie, 2010; Murano *et al.*, 2011; Takenaka *et al.*, 2011; Cui *et al.*, 2012; Ding *et al.*, 2013). Previous studies using slice preparation of guinea-pig or rat brain have reported 5-HT_{1A} receptor-mediated direct hyperpolarization of BF cholinergic neurons, probably by increasing K⁺ conductances (Khateb *et al.*, 1993; Bengston *et al.*, 2004). In this study, the holding currents were unaffected by 5-HT at the holding potential of -65mV, presumably because such K⁺ conductances were blocked by the CsCl-based internal solution.

The present findings using 5-HT receptor subtype-specific agonists and antagonists have indicated the involvement of 5-HT_{1B} receptors in the 5-HT-induced presynaptic inhibition of GABA release onto BF cholinergic neurons. 5-HT_{1B} receptor-mediated presynaptic inhibition has been reported in glutamatergic synapse in the Calyx of held (Mizutani *et al.*, 2006), glutamatergic synapse in bed nucleus of the stria terminalis (Guo & Rainnie, 2010), glutamatergic synapse in the nucleus tractus solitarius (Takenaka *et al.*, 2011), glutamatergic synapse in the deep cerebellar nuclei (Murano *et al.*, 2011), subthalamocortical glutamatergic synapse (Shengyuan *et al.*, 2013), glutamatergic synapse in the lateral habenula (Hwang & Chung, 2014). On the other hand, little has been reported on 5-HT_{1B} receptor-mediated modulation GABA release in central synapses. Activation of 5-HT_{1B} receptors in the DRN has been shown to inhibit GABA release (Lemos *et al.*, 2006).

Mechanisms independent of Ca²⁺ influx

The present results have estimated the contribution of Ca²⁺ channel subtypes involved in the GABAergic synaptic transmission onto BF cholinergic neurons, N-, P/Q and other types including R-type of Ca²⁺ channels. Unlike the previous studies (Dodge & Rahamimoff, 1967; Augustine & Charlton, 1986; Takahashi, 1992; Takahashi & Momiyama, 1993; Momiyama & Koga, 2001), the present findings indicate that the coefficient for the function between presynaptic Ca²⁺ concentration and transmitter release is less than 2, which could be a unique example among the reported synapses. Despite the physiological as well as morphological significance, the precise origins of GABAergic inputs as well as expression of Ca²⁺ channel subtypes on their terminals in BF remains unknown. A recent study has demonstrated that P/Q-type Ca²⁺ channels are expressed on the axon terminal of parvalbumin (PV)-containing interneurons in the cortex (Castejon *et al.*, 2016). PV-containing neurons are also one of the important neuronal populations in the BF, sending GABAergic inputs to cholinergic neurons (Duque *et al.*, 2000; Zaborszky & Duque, 2000). Therefore PV neurons in the BF might also express a certain subtypes of Ca²⁺ channels. Future studies using optogenetics could hopefully clarify the issues.

5-HT-induced percent inhibition of eIPSCs was not significantly different in the presence of N-, P/Q or R-type Ca²⁺ channel blockers, from that without these blockers, suggesting that 5-HT-induced effect is mediated independent of Ca²⁺ influx blockade into GABAergic presynaptic terminals. Such a

mechanism has been implied by the results on 5-HT-induced suppression of mIPSC frequency, as the effect on mIPSC frequency in nominally Ca^{2+} -free solution was not significantly different from that observed in normal external solution. The observation that the mechanisms underlying 5-HT-induced presynaptic inhibition was independent of Ca^{2+} influx modulation, have been reported by Koyama *et al.* (1999), Blackmer *et al.* (2001) and Takahashi *et al.* (2001), whereas mechanisms dependent on the modulation of Ca^{2+} influx have been also reported by other workers (Chen & Regehr, 2003; Wang *et al.*, 2003; Mizutani *et al.*, 2006; Choi *et al.*, 2007; McCamphill *et al.*, 2008).

K⁺ channel modulation

The present data suggests that 5-HT_{1B} receptor-mediated presynaptic inhibition of GABA release onto BF cholinergic neurons results from modulation of 4-AP-sensitive K⁺ channels. A recent study has reported that 5-HT_{1B} receptor-mediated presynaptic inhibition of glutamate release results from the activation of Shaker-type K⁺ channels (Hwang & Chung, 2014). As 4-AP at a concentration of 100 μM blocks broad spectrums of K⁺ channels (Ishikawa *et al.*, 2003), further studies are required to identify K⁺ channel subtypes. In addition, 4-AP blocks both presynaptic and postsynaptic K⁺ channels. Therefore, the possibility could not be excluded that 4-AP might modulate postsynaptic K⁺ channels, and that this postsynaptic effect might be one of the mechanisms underlying increased action potentials by CP93129 in current-clamp mode.

It has been reported that 5-HT_{1B} receptor subtypes are Gi/o protein-coupled, and are negatively coupled adenylyl cyclase (AC) pathway, reducing cAMP (Bouhelal *et al.*, 1988; Pytliak *et al.*, 2011). Actually, 5-HT_{1B} receptor-mediated long-term depression has been reported to be dependent on AC pathway (Mathur *et al.*, 2011). The present 5-HT_{1B} receptor-mediated effect might also depend on AC pathway. Similarly to 5-HT_{1B} receptor subtypes, dopamine D2-like receptors are also Gi/o-coupled receptors, inhibiting GABA release onto cholinergic interneurons in the striatum by directly modulating target channels via G-proteins (Momiya & Koga, 2001). This alternative pathway might also be involved in the present 5-HT_{1B} receptor-mediated effect. Detailed intracellular mechanisms including exocytotic machinery remain to be investigated as well as identifying K⁺ channel subtypes.

Physiological implications

A substantial population of BF cholinergic neurones recorded in this study project to cerebral cortex (Lehmann *et al.*, 1980; Kitt *et al.*, 1994; Jones, 2003), affecting executive functions including attention, cognition, learning and memory (for review, Miller & Cohen, 2001; Poorthuis *et al.*, 2014), as well as the control of sleep-wake states (Zant *et al.*, 2016). In addition, studies using 5-HT receptor knockout mice suggest that 5-HT receptors have a role in taking a balance between aggressiveness and sedation (Olivier *et al.*, 1994; Gingrich & Hen, 2001).

On the other hand, a number of studies in the past three decades have suggested that a considerable population of 5-HT receptor subtypes, including 5-HT_{1B} subtype, are part of the key determinants of

5-HT effects on sleep and wakefulness; 5-HT functions predominantly to promote wakefulness and to inhibit rapid-eye-movement sleep (REMS), although 5-HT also is likely to increase the propensity of sleep under certain circumstances (for review, Monti, 2011). Our present findings are consistent with these previous indications in a sense that stimulation of 5-HT_{1B} receptors would likely to upregulate cortical activity via enhancement of the cholinergic system. Further studies are required to elucidate such an elaborated system, assessing also other transmitter/receptor systems such as adenosine receptors (Hawryluk *et al.*, 2012).

In addition, a recent study has demonstrated that cholinergic projection from BF can modulate cortical responses to visual stimulation (Kimura *et al.*, 2014), as well as auditory stimulation (Letzkus *et al.*, 2011). Therefore, 5-HT_{1B} receptor-mediated inhibition of GABAergic inputs to BF cholinergic neurons could indirectly modulate such sensory processing in the cortex.

The present results on the 5-HT_{1B} receptor agonist-induced increase in action potential numbers suggest that inhibition of GABA release onto BF cholinergic neurons excite these neurons. BF nuclei also receive dense glutamatergic inputs from various brain regions (Hur *et al.*, 2009), and 5-HT could modulate glutamatergic transmission onto BF cholinergic neurons. In addition, a previous study has reported the 5-HT-induced postsynaptic membrane hyperpolarization of BF cholinergic neurons (Bengston *et al.*, 2004). Further studies are necessary to elucidate 5-HT-induced effects on glutamatergic transmission onto BF cholinergic neurones to integrate 5-HT-induced effects on both

excitatory and inhibitory transmission, thereby establishing the total modulatory roles of 5-HT in the neuronal activities of BF cholinergic neurons.

References

- Augustine, G.J. & Charlton, M.P. (1986) Calcium dependence of presynaptic calcium current and post-synaptic response at the squid giant synapse. *J. Physiol.*, **381**, 619-640.
- Bandelow, B., Zolar, J., Hollander, E., Kasper, S. & Mollar, H.J. (2008) World Federation of Societies of Biological Psychiatry (WFSBP) guidelines for the pharmacological treatment of anxiety, obsessive-compulsive and post-traumatic stress disorders-first version. *World J. Biol. Psychia.*, **9**, 248-312.
- Bengston, C.P., Lee, D.J. & Osborne, P.B. (2004) Opposing electrophysiological actions of 5-HT on noncholinergic and cholinergic neurons in the rat ventral pallidum *in vitro*. *J. Neurophysiol.*, **92**, 433-443.
- Blackmer, T., Larsen, E.C., Takahashi, M., Martin, T.F.J., Alford, S. & Hamm, H.E. (2001) G protein $\beta\gamma$ subunit-mediated presynaptic inhibition: regulation of exocytotic fusion downstream of Ca^{2+} entry. *Science*, **292**, 293-297.
- Bouhelal, R., Smounya, L. & Bockaert, J. (1988) 5-HT_{1B} receptors are negatively coupled with adenylate cyclase in the rat substantia nigra. *Eur. J. Pharmacol.*, **151**, 189-196.

- Castejon, C., Barros-Zulaica, N. & Nuñez A. (2016) Control of somatosensory cortical processing by thalamic posterior medial nucleus: a new role of thalamus in cortical function. *PLoS One*, **11**, e0148169.
- Chang, H.T., Tian, Q. & Herron, P. (1995) GABAergic axons in the ventral forebrain of the rat: an electron microscopic study. *Neuroscience*, **68**, 207-220.
- Chen, C. & Regehr, W.G. (2003) Presynaptic modulation of the retinogeniculate synapse. *J. Neurosci.*, **23**, 3130-3135.
- Choi, I.S., Cho, J.H., Kim, J.T., Park, E.J., Lee, M.G., Shin, H.I., Choi, B.J. & Jang, I.S. (2007) Serotonergic modulation of GABAergic synaptic transmission in developing rat CA3 pyramidal neurons. *J. Neurochem.*, **103**, 2342-2353.
- Coyle, J.T., Price, D.L. & DeLong, M.R. (1983) Alzheimer's disease: a disorder of cortical cholinergic innervation. *Science*, **219**, 1184-1190.
- Cui, R.J., Roberts, B.L., Zhao, H., Zhu, M. & Appleyard, S.M. (2012) Serotonin activates catecholamine neurons in the solitary tract nucleus by increasing spontaneous glutamate inputs. *J. Neurosci.*, **32**, 16530-16538.
- Daubert, E.A. & Condron, B.G. (2010) Serotonin: a regulator of neuronal morphology and circuitry. *Trends Neurosci.*, **33**, 424-434.
- Ding, S., Li, L. & Zhou, F.-M. (2013) Presynaptic serotonergic gating of the subthalamopnigral glutamatergic projection. *J. Neurosci.*, **33**, 4875-4885.

- Dodge, F.A. & Rahamimoff, R. (1967) Co-operative action of calcium ions in transmitter release at the neuromuscular junction. *J. Physiol.*, **193**, 419-432.
- Duque, A., Balatoni, B., Detari, L. & Zaborszky L. (2000). EEG correlation of the discharge properties of identified neurons in the basal forebrain. *J. Neurophysiol.*, **84**, 1627-1635.
- Fukushima, T., Ohtsubo, T., Tsuda, M., Yanagawa, Y. & Hori, Y. (2009) Facilitatory actions of serotonin type 3 receptors on GABAergic inhibitory synaptic transmission in the spinal superficial dorsal horn. *J. Neurophysiol.*, **102**, 1459-1471.
- Gasbarri, A., Sulli, A., Pacitti, C. & McGaugh, L. (1999) Serotonergic input to cholinergic neurons in the substantia innominate and nucleus basalis magnocellularis in the rat. *Neuroscience*, **91**, 1129-1142.
- Gingrich, J.A. & Hen, R. (2001) Dissecting the role of the serotonin system in neuropsychiatric disorders using knockout mice. *Psychopharmacology*, **155**, 1-10.
- Guo, J.-D. & Rainnie, D.G. (2010) Presynaptic 5-HT_{1B} receptor-mediated serotonergic inhibition of glutamate transmission in the bed nucleus of the stria terminalis. *Neuroscience*, **165**, 1390-1401.
- Hannon, J. & Hoyer, D. (2008) Molecular biology of 5-HT receptors. *Behav. Brain Res.*, **195**, 198-213.
- Hawryluk, J.M., Ferrari, J.J., Keating, S.A. & Arrigoni, E. (2012) Adenosine inhibits glutamatergic input to basal forebrain cholinergic neurons. *J. Neurophysiol.*, **107**, 2769-2781.
- Heimer, L., Zahm, D.S., Churchill, L., Kalivas, P.W. & Wohtmann, C. (1991) Specificity in the projection patterns of accumbal core and shell in the rat. *Neuroscience*, **41**, 89-125.

- Hori, Y., Endo, K. & Takahashi, T. (1996) Long-lasting synaptic facilitation induced by serotonin in superficial dorsal horn neurones of the rat spinal cord. *J. Physiol.*, **492**, 867-876.
- Hur, E.E., Edwards, R.H., Rommer, E. & Zaborszky, L. (2009) Vesicular glutamate transporter 1 and vesicular glutamate transporter 2 synapses on cholinergic neurons in the sublenticular gray of the rat basal forebrain: a double label electron microscopic study. *Neuroscience*, **164**, 1721-1731.
- Hwang, E.-K. & Chung, J.-M. (2014) 5HT_{1B} receptor-mediated pre-synaptic depression of excitatory inputs to rat lateral habenula. *Neuropharmacology*, **81**, 153-165.
- Ishikawa, T., Nakamura, Y., Saitoh, N., Li, W-B., Iwasaki, S. & Takahashi T. (2003) Distinct roles of Kv1 and Kv3 potassium channels at the Calyx of Held presynaptic terminal. *J. Neurosci.*, **23**, 10445-10453.
- Jones, B.E. (2003) Arousal systems. *Front. Biosci.*, **8**, 438-451.
- Khateb, A., Fort, P., Alonso, A., Jones, B.E. & Mühlethaler, M. (1993) Pharmacological and immunohistochemical evidence for serotonergic modulation of cholinergic nucleus basalis neurons. *Eur. J. Neurosci.*, **5**, 541-547.
- Kimura, R., Safari, M.-S., Mirnajafi-Zadeh, J., Kimura, R., Ebina, T., Yanagawa, Y. & Tsumoto, T. (2014) Curtailing effect of awakening on visual responses of cortical neurons by cholinergic activation of inhibitory circuits. *J. Neurosci.*, **34**, 10122-10133.
- Kitt, C.A., Höhmann, C., Coyle, J.T. & Price, D.L. (1994) Cholinergic innervations of mouse forebrain structures. *J. Comp. Neurol.*, **341**, 117-129.

- Koyama, S., Kubo, C., Rhee, J.-S. & Akaike, N. (1999). Presynaptic serotonergic inhibition of GABAergic synaptic transmission in mechanically dissociated rat basolateral amygdala neurons. *J. Physiol.*, **518**, 525-538.
- Lehmann, J., Nagy, J.I., Atmadia, S. & Fibiger, H.C. (1980) The nucleus basalis magnocellularis: the origin of a cholinergic projection to neocortex of the rat. *Neuroscience*, **5**, 1161-1174.
- Lemos, J.C., Pan, Y.Z., Ma, X., Lamy, C., Akanwa, A.C. & Beck, S.G. (2006) Selective 5-HT_{1B} receptor inhibition of glutamatergic and gabaergic synaptic activity in the rat dorsal and median raphe. *Eur. J. Neurosci.*, **24**, 3415-3430.
- Letzkus, J.J., Wolff, S.B.E., Meyer, E.M.M., Tovote, P., Courtin, J. & Herry, C. (2011) A disinhibitory microcircuit for associative fear learning in the auditory cortex. *Nature*, **480**, 331-335.
- Lowry, C.A., Johnson, P.L., Hay-Schmidt, A., Mikkelsen, J. & Shekhar, A. (2005) Modulation of anxiety circuits by serotonergic systems. *Stress*, **8**, 233-246.
- Mathur, B.N., Capik, N.A., Alvarez, V.A. & Lovinger, D.M. (2011) Serotonin induces long-term depression at corticostriatal synapses. *J. Neurosci.*, **31**, 7402-7411.
- McCamphill, P.K., Dunn, T.W. & Syed, N.I. (2008) Serotonin modulates transmitter release at central *Lymnaea* synapses through G-protein-coupled and cAMP-mediated pathway. *Eur. J. Neurosci.*, **27**, 2033-2042.
- Miller, E.F. & Cohen, J.D. (2001) An integrative theory of prefrontal function. *Annu. Rev. Neurosci.*, **24**, 167-202.

- Mizutani, H., Hori, T. & Takahashi, T. (2006) 5-HT_{1B} receptor-mediated presynaptic inhibition at the calyx of Held of immature rats. *Eur. J. Neurosci.*, **24**, 1946-1954.
- Momiyama, T. & Fukazawa, Y. (2007) D1-like dopamine receptors selectively block P/Q-type calcium channels to reduce glutamate release onto cholinergic basal forebrain neurones of immature rats. *J. Physiol.*, **580**, 103-117.
- Momiyama, T. & Koga, E. (2001) Dopamine D₂-like receptors selectively block N-type Ca²⁺ channels to reduce GABA release onto rat striatal cholinergic interneurons. *J. Physiol.*, **533**, 479-492.
- Momiyama, T. & Sim, J.A. (1996) Modulation of inhibitory transmission by dopamine in rat basal forebrain nuclei: activation of presynaptic D1-like dopaminergic receptors. *J. Neurosci.*, **16**, 7505-7512.
- Momiyama, T. & Zaborszky, L. (2006) Somatostatin presynaptically inhibits both GABA and glutamate release onto rat basal forebrain cholinergic neurons. *J. Neurophysiol.*, **96**, 686-694.
- Monti, J.M. (2011) Serotonin control of sleep-wake behavior. *Sleep Med. Rev.*, **15**, 269-281.
- Murano, M., Saitow, F. & Suzuki, H. (2011) Modulatory effects of serotonin on glutamatergic synaptic transmission and long-term depression in the deep cerebellar nuclei. *Neuroscience*, **172**, 118-128.
- Olivier, B., Molewijk, E., van Oorschot, R., van der Poel, G., Zethof, T., van der Heyden, J. & Mos, J. (1994) New animal models of anxiety. *Eur. Neuropsychopharm.*, **4**, 93-102.
- Oyanagi, K., Takahashi, H., Wakabayashi, K. & Ikura, F. (1989) Correlative decrease of large neurons in the neostriatum and basal nucleus of Meynert in Alzheimer's disease. *Brain Res.*, **504**, 354-357.

- Poorthuis, R.B., Enke, L. & Letzkus, J.J. (2014) Cholinergic circuit modulation through differential recruitment of neocortical interneuron types during behaviour. *J. Physiol.*, **592**, 4155-4164.
- Pytliak, M., Vargová, V., Mechírová, V. & Felšöci, M. (2011) Serotonin receptors-from molecular biology to clinical applications. *Physiol. Res.*, **60**, 15-25.
- Ressler, K.J. & Nemeroff, C.B. (2000) Role of serotonergic and noradrenergic systems in the pathophysiology of depression and anxiety disorders. *Depress. Anxiety*, **12** (Suppl 1), 2-19.
- Rye, D.B., Wainer, B.H., Mesulum, M.-M., Mufson, E.J. & Saper, C.B. (1984) A study of cholinergic and noncholinergic components employing retrograde tracing and immunohistochemical localization of choline acetyltransferase. *Neuroscience*, **13**, 627-643.
- Sari, Y., Miquel, M.-C., Brisorgueil, M.-J., Ruiz, G., Doucet, E., Hamon, M. & Verge, D. (1999) Cellular and subcellular localization of 5-hydroxytryptamine_{1B} receptors in the rat central nervous system: immunocytochemical, autoradiographic and lesion studies. *Neuroscience*, **88**, 899-915.
- Shengyuan, D., Li, L. & Zhou, F.-M. (2013) Presynaptic serotonergic gating of the subthalamopnigral glutamatergic projection. *J. Neurosci.*, **33**, 4875-4885.
- Sun, N. & Cassell, M.D. (1993) Intrinsic GABAergic neurons in the rat central extended amygdala. *J. Comp. Neurol.*, **330**, 381-404.
- Takahashi, M., Freed, R., Blackmer, T. & Alford, S. (2001) Calcium influx-independent depression of transmitter release by 5-HT at lamprey spinal cord synapses. *J. Physiol.*, **532**, 323-336.

- Takahashi, T. (1992) The minimal inhibitory synaptic currents evoked in neonatal rat motoneurons. *J. Physiol.*, **450**, 593-611.
- Takahashi, T. & Momiyama, A. (1993) Different types of calcium channels mediate central synaptic transmission. *Nature*, **366**, 156-158.
- Takenaka, R., Ohi, Y. & Haji, A. (2011) Distinct modulatory effects of 5-HT on excitatory synaptic transmission in the nucleus tractus solitaries of the rat. *Eur. J. Pharmacol.*, **671**, 45-52.
- Umemiya, M. & Berger, A.J. (1995) Presynaptic inhibition by serotonin of glycinergic inhibitory synaptic currents in the rat brain stem. *J. Neurophysiol.*, **73**, 1192-1201.
- Wang, S.-J., Su, C.-F. & Kuo, Y.-H. (2003) Fluoxetine depresses glutamate exocytosis in the rat cerebrocortical nerve terminals (synaptosomes) via inhibition of P/Q-type Ca²⁺ channels. *Synapse*, **48**, 170-177.
- Wu, M., Shanabrough, M., Leranth, C. & Alreja, M. (2000) Cholinergic excitation of septohippocampal GABA but not cholinergic neurons: implications for learning and memory. *J. Neurosci.*, **15**, 3900-3908.
- Zaborszky, L. & Culliman, W.E. (1992) Projections from the nucleus accumbens to cholinergic neurons of the ventral pallidum: a correlated light and electron microscopic double-immunolabeling study in rat. *Brain Res.*, **570**, 92-101.
- Zaborszky, L. & Duque, A. (2000) Local synaptic connections of basal forebrain neurons. *Behav. Brain Res.*, **115**, 143-158.

Zaborszky, L, Heimer, L., Eckenstein, F. & Lenanth, C. (1986) GABAergic input to cholinergic forebrain neurons: an ultrastructural study using retrograde tracing of HRP and double immunolabeling. *J. Comp. Neurol.*, **250**, 282-295.

Zant, J.C., Kim, T., Prokai, L., Szarka, S., McNally, J., McKenna, J.T., Shukla, C., Yang, C., Kalinchuk, A.V., McCarley, R.W., Brown, R.E. & Basheer R. (2016) Cholinergic neurons in the basal forebrain promote wakefulness by actions on neighboring non-cholinergic neurons: an opto-dialysis study. *J. Neurosci.*, **36**, 20547-2067.

Figure legends.

FIG. 1. Labeling of a cholinergic neuron in the basal forebrain (BF) using Cy3-192IgG, a selective marker of p75-receptor-expressing neurones, and blockade of the evoked synaptic currents by bicuculline.

A: A BF neuron viewed under IR-DIC microscopy. Calibration, 20 μm . **B:** The same neuron as in A in a fluorescent image labelled with Cy3-192IgG. **C1:** Time course of blockade of the evoked synaptic currents by bicuculline (10 μM). Synaptic currents were evoked by focal stimulation in the presence of CNQX (5 μM), strychnine (0.5 μM), and D-AP5 (25 μM), to block non-NMDA glutamatergic, glycinergic, and NMDA glutamatergic components respectively. Holding potential was -65 mV. Each

point in the time course shows the amplitude of the synaptic currents evoked at 0.2 Hz (every 5 s). Bicuculline applied in the bath during the indicated period reversibly blocked the synaptic currents. **C2:** Superimposed averaged traces of 20 consecutive synaptic currents during the indicated periods in the time course plot. Blockade by bicuculline suggests that these synaptic currents are γ -aminobutyric acid type A (GABA_A)-receptor-mediated inhibitory postsynaptic currents (IPSCs).

FIG. 2. Inhibitory effect of 5-HT on GABAergic eIPSCs

Synaptic currents were evoked at a rate of 0.2 Hz in the presence of CNQX (5 μ M), strychnine (0.5 μ M) and D-AP5 (25 μ M), to block non-NMDA glutamatergic, glycinergic and NMDA glutamatergic components respectively. Holding potential was -65 mV. **A:** Time course of inhibition of the eIPSCs by 5-HT (1 μ M) and recovery on washout. Bath application of 5-HT (1 μ M) during the indicated period gradually suppressed the eIPSCs and the effect reached a steady state in 2 min. eIPSCs recovered from 5-HT-induced inhibition after 10-min washout. Superimposed traces on the right show averages of 20 consecutive eIPSCs during the indicated periods in the time course plot. **B:** Concentration-dependent inhibition of eIPSCs by 5-HT. Numbers of cells are shown in parentheses. Error bars indicate SEM. The data were fitted to a logistic function to estimate the IC₅₀ value (1.89 μ M), maximum inhibition (65.0%) and Hill slope (1.04).

FIG. 3. Effect of 5-HT receptor agonists on eIPSCs

All IPSCs were evoked at 0.2 Hz in the presence of CNQX (5 μ M), strychnine (0.5 μ M) and D-AP5 (25 μ M). The holding potential was -65 mV. **A:** Time course of lack of effect of a 5-HT_{1A} receptor agonist, 8-OH-DPAT. 8-OH-DPAT (10 μ M) was applied in the bath during the indicated period. Superimposed traces on the right show averages of 20 consecutive eIPSCs during the indicated periods in the time course plot. **B:** Time course of inhibitory effect of a 5-HT_{1B} receptor agonist, CP93129 (1 μ M). CP93129 (1 μ M) was applied in the bath during the indicated period. Superimposed traces on the right show averages of 20 consecutive eIPSCs during the indicated periods in the time course plot. **C:** Histograms summarizing the mean inhibitory effect of 5-HT, CP93129 and 8-OH-DPAT at a concentration of 10 μ M. Error bars indicate SEM. Inhibition by 10 μ M 5-HT and 10 μ M CP93129 were $58.2 \pm 2.14\%$ (n = 46) and $52.5 \pm 5.50\%$ (n = 11) respectively. These were significantly (**P* = 0.0003) larger than that of 10 μ M 8-OH-DPAT ($11.2 \pm 6.12\%$, n = 6). Inhibition by 1 μ M CP93129 was $67.6 \pm 7.13\%$ (n = 5), which was significantly (**P* = 0.006) larger than that by 1 μ M 5-HT ($34.7 \pm 4.45\%$, n = 8).

FIG. 4. Effect of 5-HT receptor antagonists on 5-HT-induced inhibition of eIPSCs

Effect of 5-HT (10 μ M) on IPSCs in the presence of a 5-HT_{1B} receptor antagonist, NAS-181 (30 μ M, A), or a 5-HT_{1A} receptor antagonist, NAN-190 (30 μ M, B), was compared with that of 5-HT alone. **A and B:** Time course of 5-HT (10 μ M)-induced effect before and after application of NAS-181 (A) or NAN-190 (B). 5-HT and antagonist were applied during the indicated periods. Superimposed traces

on the right are averages of 20 consecutive eIPSCs during the indicated periods in the time course plot.

C: The concentration-response curves in the absence and presence of NAS-181 are superimposed in the graphs. The concentration-response curve was shifted to the right by NAS-181 (filled circles) with the estimated IC_{50} value, maximum inhibition and Hill slope being 33.4 μ M, 61.6% and 2.31 respectively. Curve in the absence of NAS-181 (open squares) is same as in Fig. 2B. Error bars indicate SEM and numbers of cells examined are given in parentheses. From this shift, an apparent K_B value for NAS-181 was calculated to be 0.70 μ M (pK_B 6.2).

FIG. 5. Effect of 5-HT on spontaneous mIPSCs

mIPSCs were recorded in 2.4 mM CaCl-containing external solution in the presence of tetrodotoxin (TTX, 0.5 μ M) in addition to CNQX (5 μ M), strychnine (0.5 μ M) and D-AP5 (25 μ M). Holding potential was -65 mV. **A:** Consecutive traces recorded before and 3 min after application of 1 μ M 5-HT. **B and C:** Cumulative probability distribution of inter-event intervals (B) and peak amplitudes (C) of mIPSCs constructed from the same neuron shown in A, comparing distributions in the absence (open symbols) and presence (filled symbols) of 5-HT. Control data contain 263 events per 3 min period, whereas data in the presence of 5-HT contain 91 events per 3 min period. The inter-event interval was significantly ($P = 0.00000006$, K-S test) increased, whereas the distribution of mIPSC amplitude was unaffected by 5-HT, suggesting that 5-HT presynaptically inhibits GABA release. **D:** Averaged mIPSCs in control (263 events) and during application of 5-HT (91 events). Mean amplitude

of mIPSCs in control and in the presence of 5-HT were 49.9 and 47.3 pA, respectively. **E:** Histograms summarizing the inhibitory effect of 5-HT (1 μ M) on the frequency of mIPSCs in external Ca^{2+} concentrations of 2.4 and 0 mM. 5-HT-induced inhibition of mIPSC frequency in 2.4 mM Ca^{2+} and Ca^{2+} -free solutions were $52.9 \pm 11.6\%$ ($n = 6$) and $41.1 \pm 10.4\%$ ($n = 6$) respectively. The effect in the nominally Ca^{2+} -free solution was not significantly ($P = 0.463$) different from that in 2.4 mM Ca^{2+} solution.

FIG. 6. CP93829-induced increase in paired-pulse ratio (PPR)

A: Traces averaged 20 consecutive IPSCs evoked with a paired-pulse protocol (interspike interval of 50 ms) at a rate of 0.2 Hz in control and during application of CP93129 (10 μ M). PPR was calculated from the equation of $\text{IPSC}_2/\text{IPSC}_1$, where IPSC_1 and IPSC_2 correspond to the peak amplitude of the first and second IPSCs respectively. **B:** Summarized histogram showing the change in mean PPR. PPR was significantly ($P = 0.007$) increased from 0.75 ± 0.05 ($n = 8$) to 1.16 ± 0.12 by application of CP93129 (10 μ M).

FIG. 7. Suppression of the eIPSCs by ω -CgTX and ω -Aga-TK

A and B: Time course of the inhibitory effects of ω -CgTX (3 μ M, A) and ω -Aga-TK (200 nM, B) on the amplitude of eIPSCs. Toxins were bath applied during the indicated periods. **A:** ω -CgTX reduced the amplitude of eIPSCs by 55.6% of control. **B:** ω -Aga-TK reduced the amplitude of eIPSCs by 49.9%

of control. Subsequent application of ω -Aga-TK (A) or ω -CgTX (B) almost blocked the remaining eIPSCs. Superimposed current traces at the right of A and B are the averages of 20 consecutive eIPSCs during the indicated periods. **C:** Bar graphs summarizing the suppression of the IPSCs by ω -CgTX (3 μ M), ω -Aga-TK (200 nM) and SNX-482 (300 nM). Values for ω -CgTX, ω -Aga-TK, both ω -CgTX and ω -Aga-TK, and SNX-482 are $60.1 \pm 4.85\%$ (n = 9), $47.4 \pm 7.52\%$ (n = 10), $89.7 \pm 3.66\%$ (n = 6) and 7.41 ± 5.07 (n = 13) respectively.

FIG. 8. Effects of ω -CgTX, ω -Aga-TK or SNX-482 on 5-HT-induced inhibition of eIPSCs

A and B: Time course of 5-HT (10 μ M)-induced effect before and after application of ω -CgTX (3 μ M, A) or ω -Aga-TK (200 nM, B). 5-HT, ω -CgTX and ω -Aga-TK were applied in the bath during the indicated periods. Toxins were applied after eIPSCs had recovered from the inhibition induced by the initial application of 5-HT. After the suppression by ω -CgTX or ω -Aga-TK had reached steady state, 5-HT was applied again in the presence of the toxin. Superimposed traces on the right are averages of 20 consecutive eIPSCs during the indicated periods in the time course plot. **C:** Bar graphs summarizing the inhibitory effect of 5-HT in the absence and presence of Ca^{2+} channel blockers. 5-HT-induced inhibitory effect in the presence of ω -CgTX ($53.0 \pm 6.92\%$, n = 6) was not significantly different from that of 5-HT alone in the corresponding neurons ($61.8 \pm 6.99\%$, n = 6). Similarly, 5-HT-induced inhibitory effect in the presence of ω -Aga-TK ($62.8 \pm 11.1\%$, n = 7) was not significantly different from that of 5-HT alone in the corresponding neurons ($57.3 \pm 4.98\%$, n = 7), and 5-HT-induced

inhibitory effect in the presence of SNX-482 ($68.5 \pm 6.12\%$, $n = 5$) was also not significantly different from that of 5-HT alone in the corresponding neurons ($58.8 \pm 5.25\%$, $n = 5$).

FIG. 9. Effect of 4-AP on CP93129-induced inhibition of eIPSCs

A: Time course of the effect of CP93129 ($10 \mu\text{M}$)-induced effect on the eIPSCs before and after application of 4-AP ($100 \mu\text{M}$). Drugs were applied in the bath during the indicated periods. 4-AP was applied after eIPSCs had recovered from the inhibition induced by the initial application of CP93129. After the enhancing effect of 4-AP had reached steady state, CP93129 was applied again in the presence of 4-AP. Superimposed traces on the right are averages of 20 consecutive eIPSCs during the indicated periods in the time course plot. **B:** Histograms showing the enhancing effect of 4-AP on the amplitude of eIPSCs. Application of 4-AP without pre-application of CP93129 increased the eIPSC amplitude to $204.3 \pm 31.7\%$ ($n = 6$) of the value before 4-AP application (middle histogram). Application of 4-AP after washout of CP93129 increased the eIPSC amplitude to $212.1 \pm 50.5\%$ ($n = 6$, right histogram), that was not significantly ($P = 0.901$) different from the value without pre-application of CP93129. **C:** Histograms showing the effect of 4-AP on the CP93129-induced inhibition of eIPSCs. CP93129-induced inhibitory effect was significantly ($P = 0.0005$) decreased to $8.51 \pm 2.87\%$ ($n = 12$) from the value without 4-AP ($46.3 \pm 6.10\%$, $n = 6$). Numbers in parentheses indicate number of neurons examined.

FIG. 10. Effect of CP93129 on firings of BF cholinergic neurons

A: Membrane responses by hyperpolarizing and depolarizing current injections before drug application (a), during application of CP93129 (10 μ M, b) and 10 min washout of the drug (c). CP93129 had no effect on the membrane potential. Note that the number of action potentials at the most depolarized potential increased from 2 to 4 by the agonist, whereas at the second depolarized potential, 3 action potentials were induced during agonist application compared to the lack of action potential generation before agonist application. The apparent synaptic potentials observed at the hyperpolarizing potentials were blocked by bicuculline (not shown). **B:** Change in the number of action potentials generated at the most depolarized potential by application of CP93129 in each of the examined neurons. Mean values with SEM are indicated by horizontal bars. The value was 4.74 ± 0.62 (n = 19) in control, that was significantly ($P = 0.006$) increased to 5.42 ± 0.62 (n = 19) by application of CP93129.

Figure 1

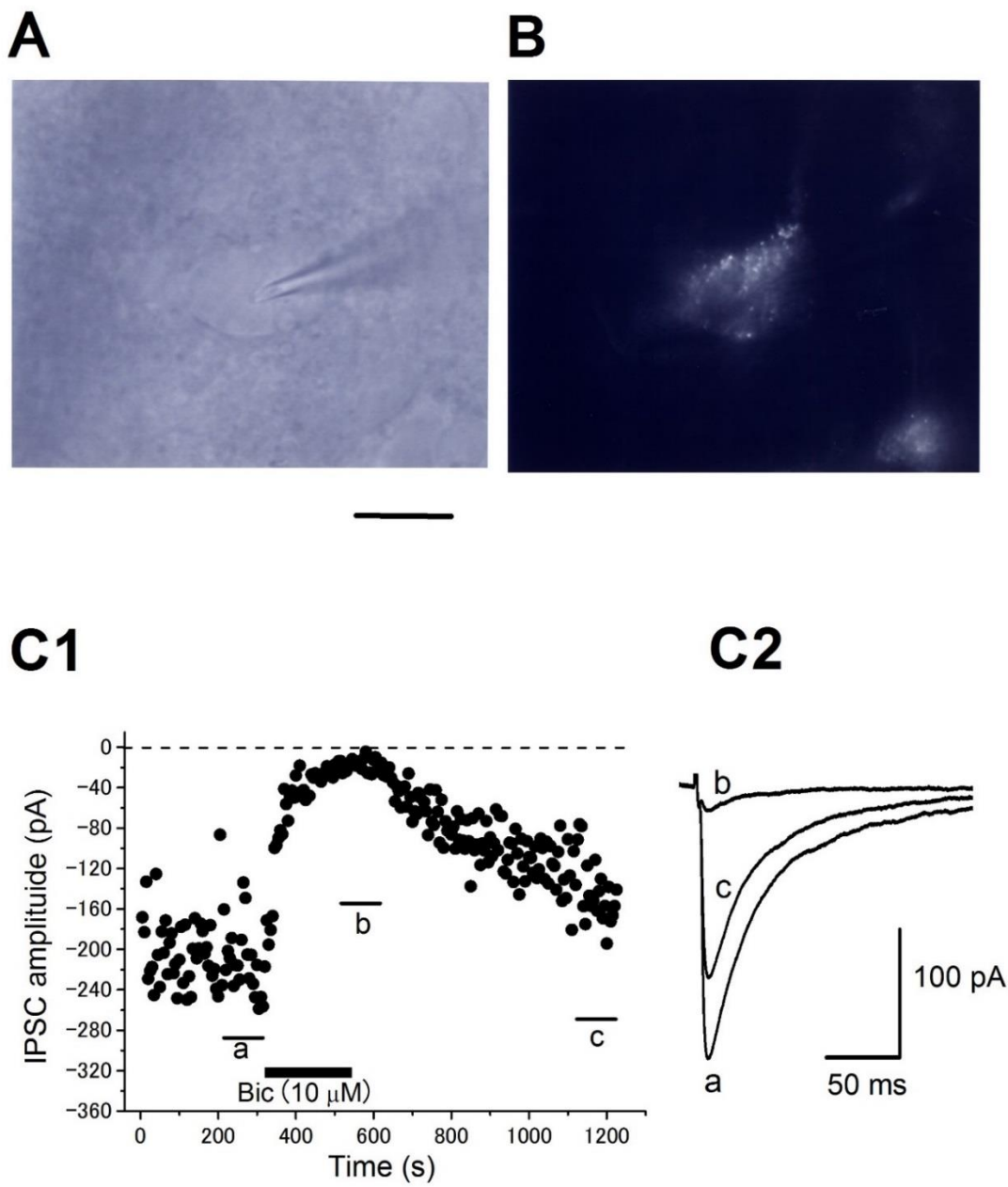


Figure 2

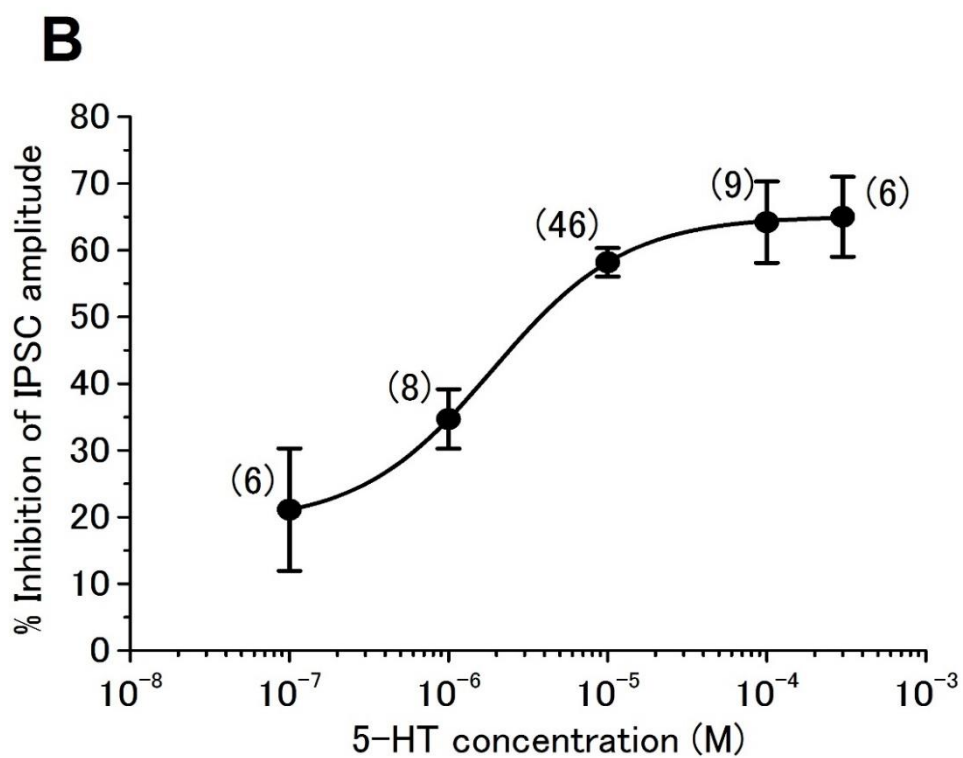
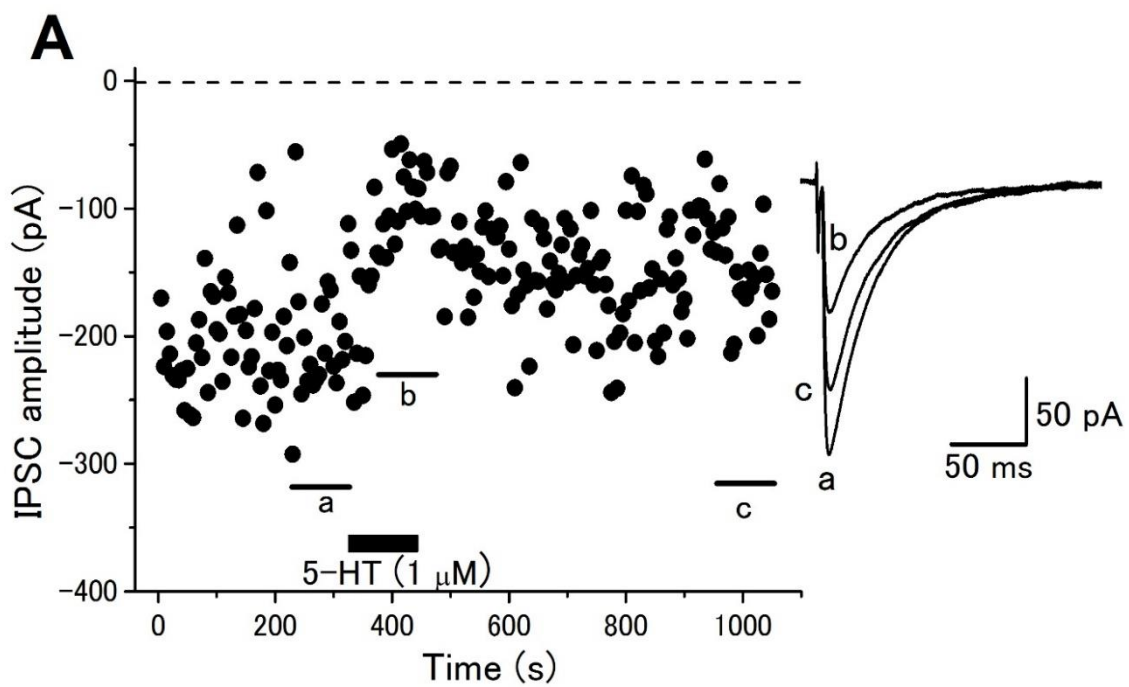


Figure 3

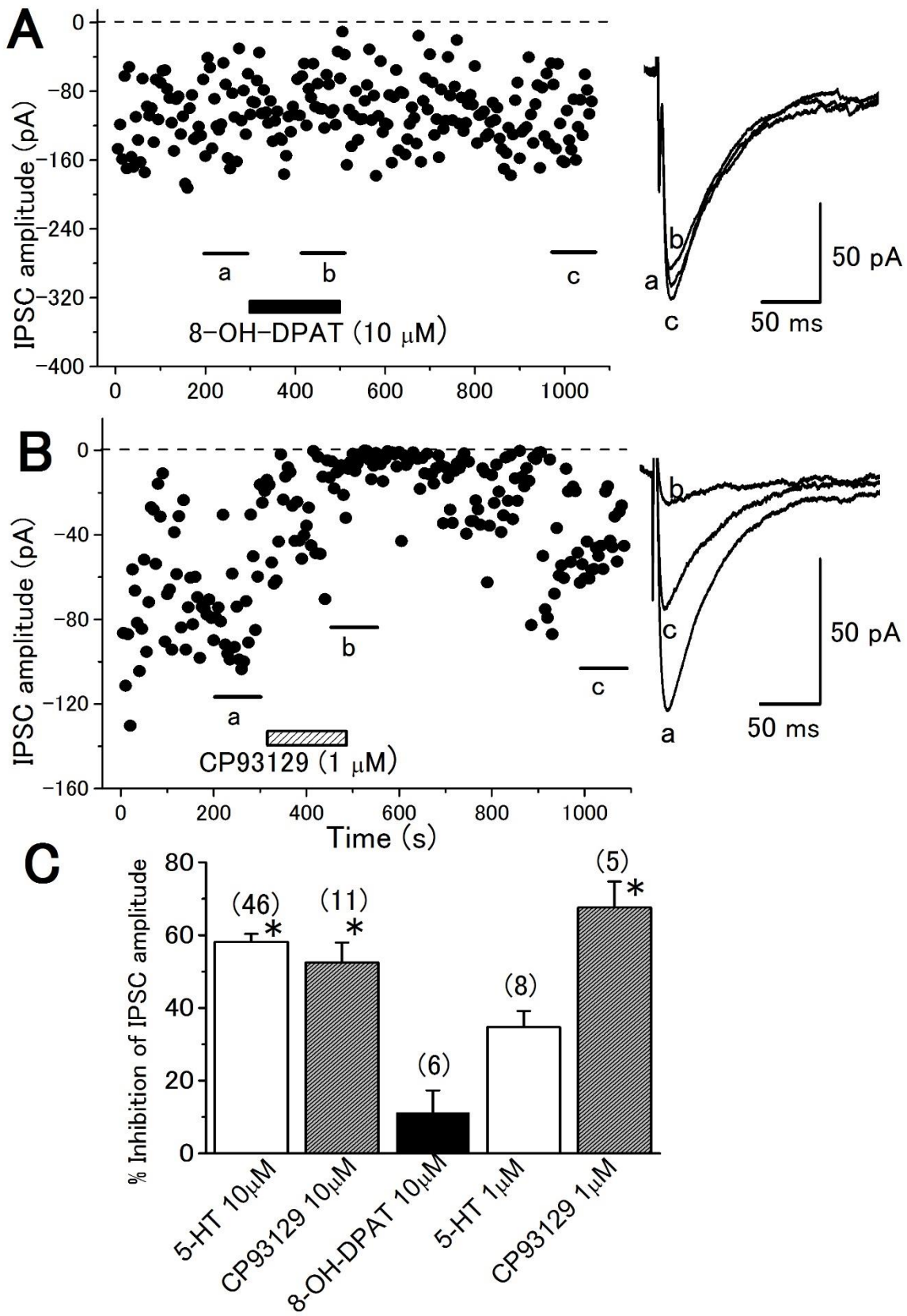


Figure 4

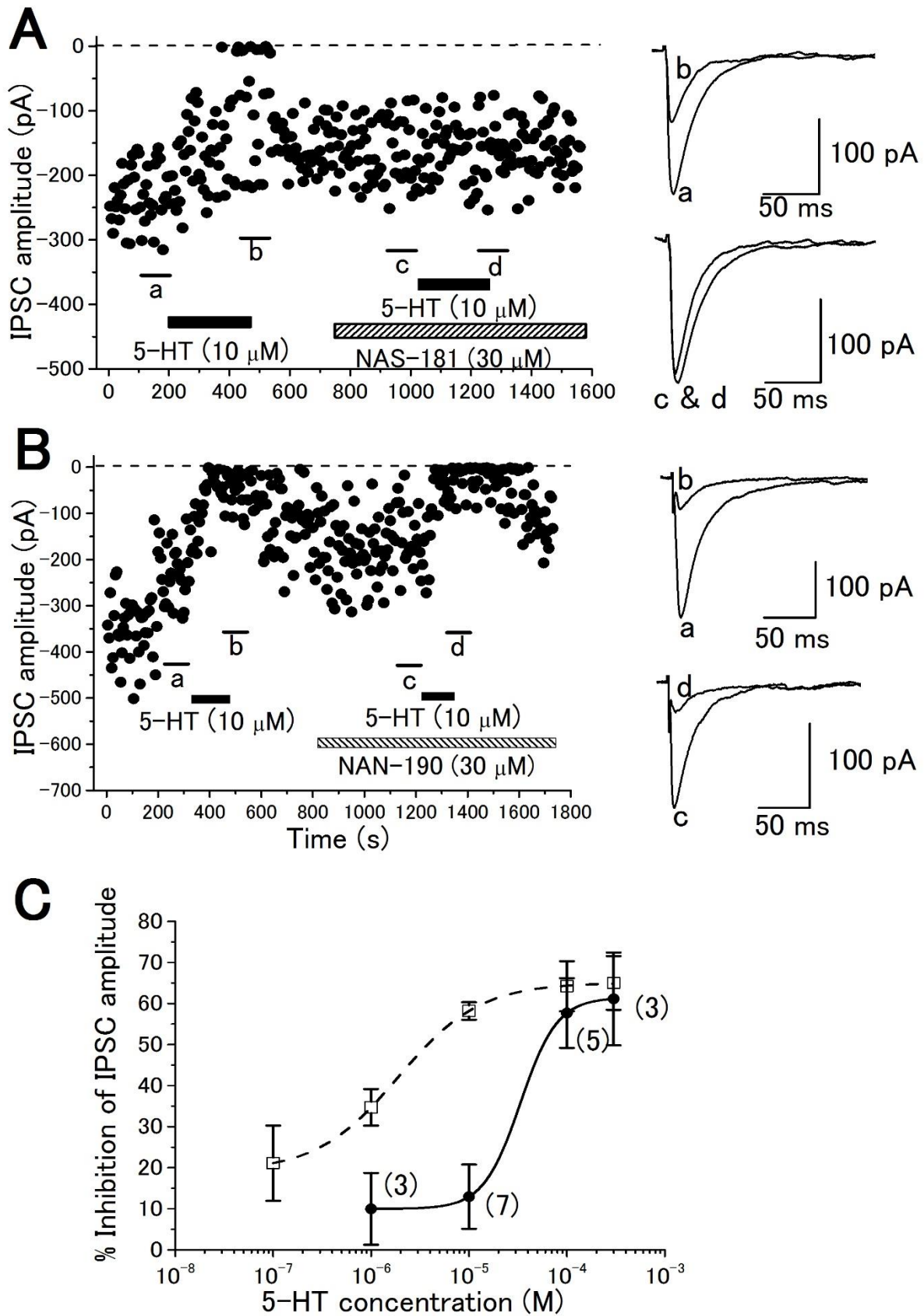


Figure 5

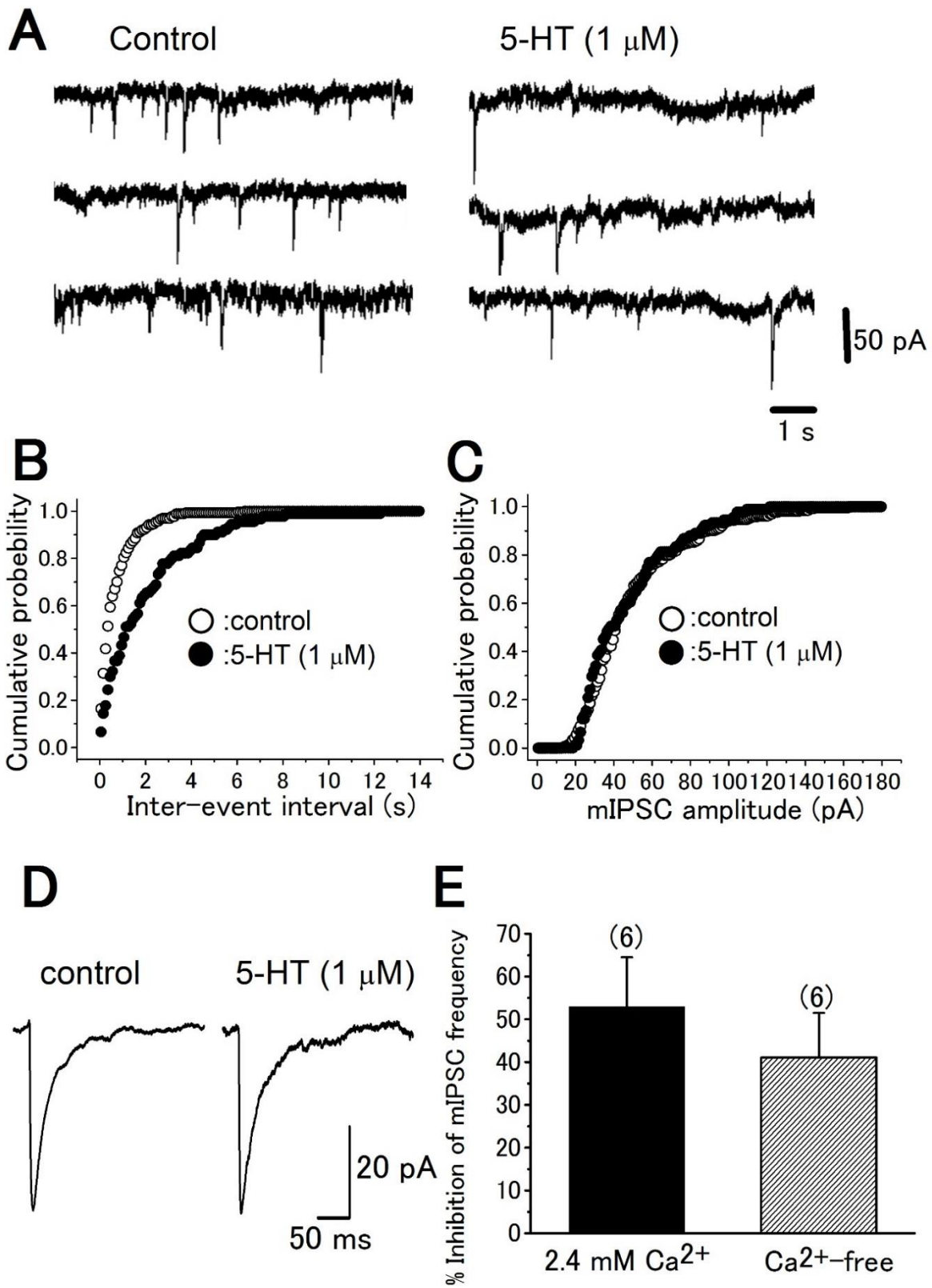


Figure 6

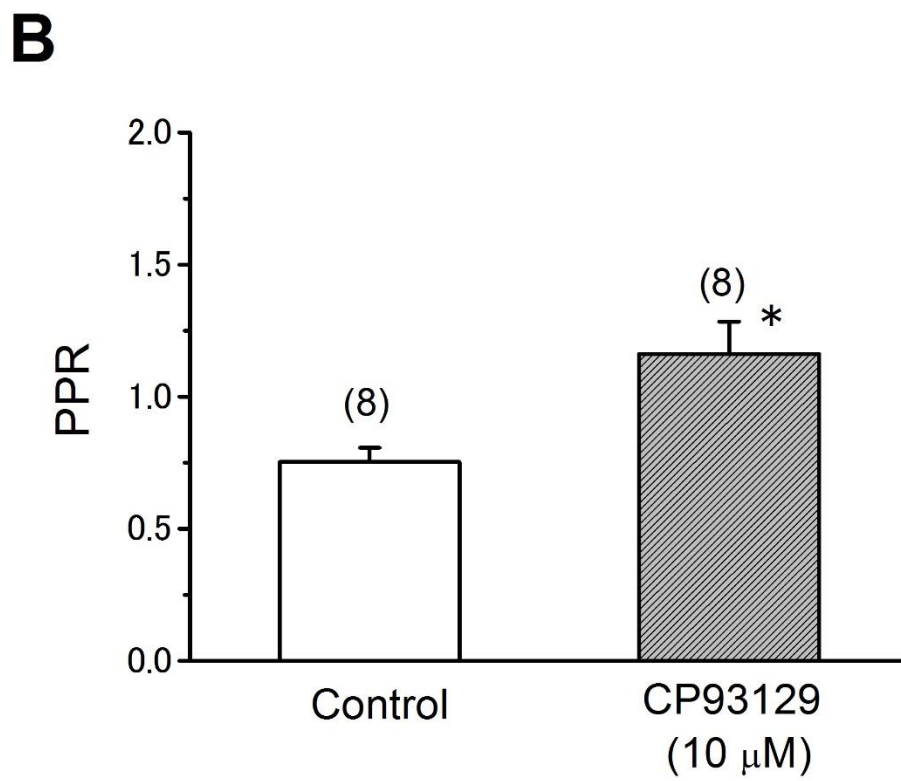
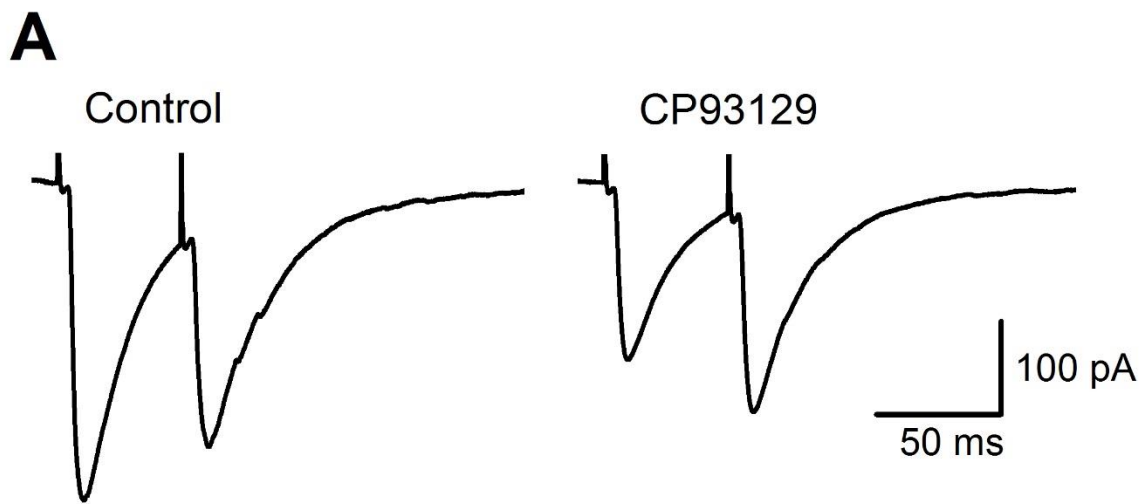


Figure 7

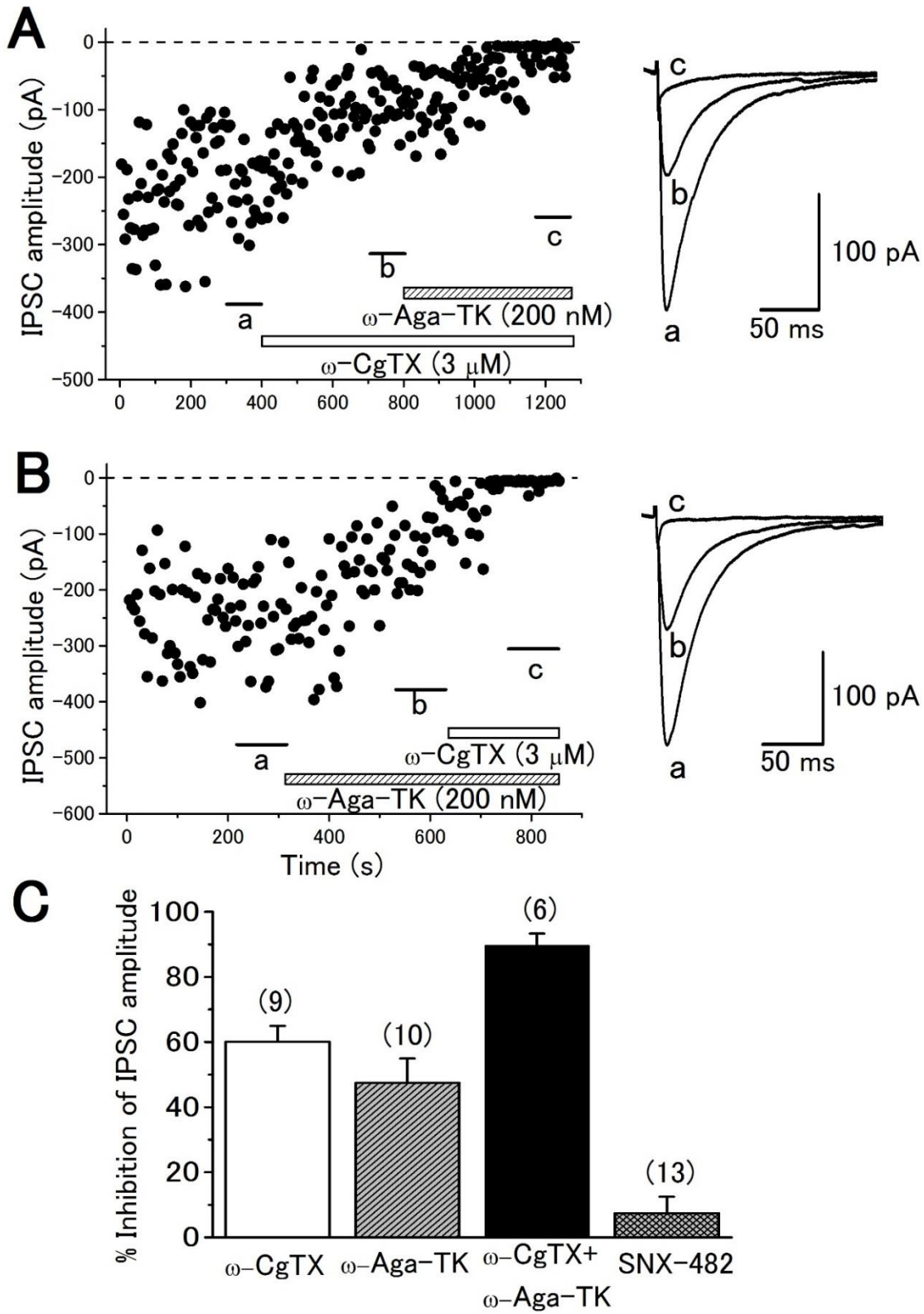


Figure 8

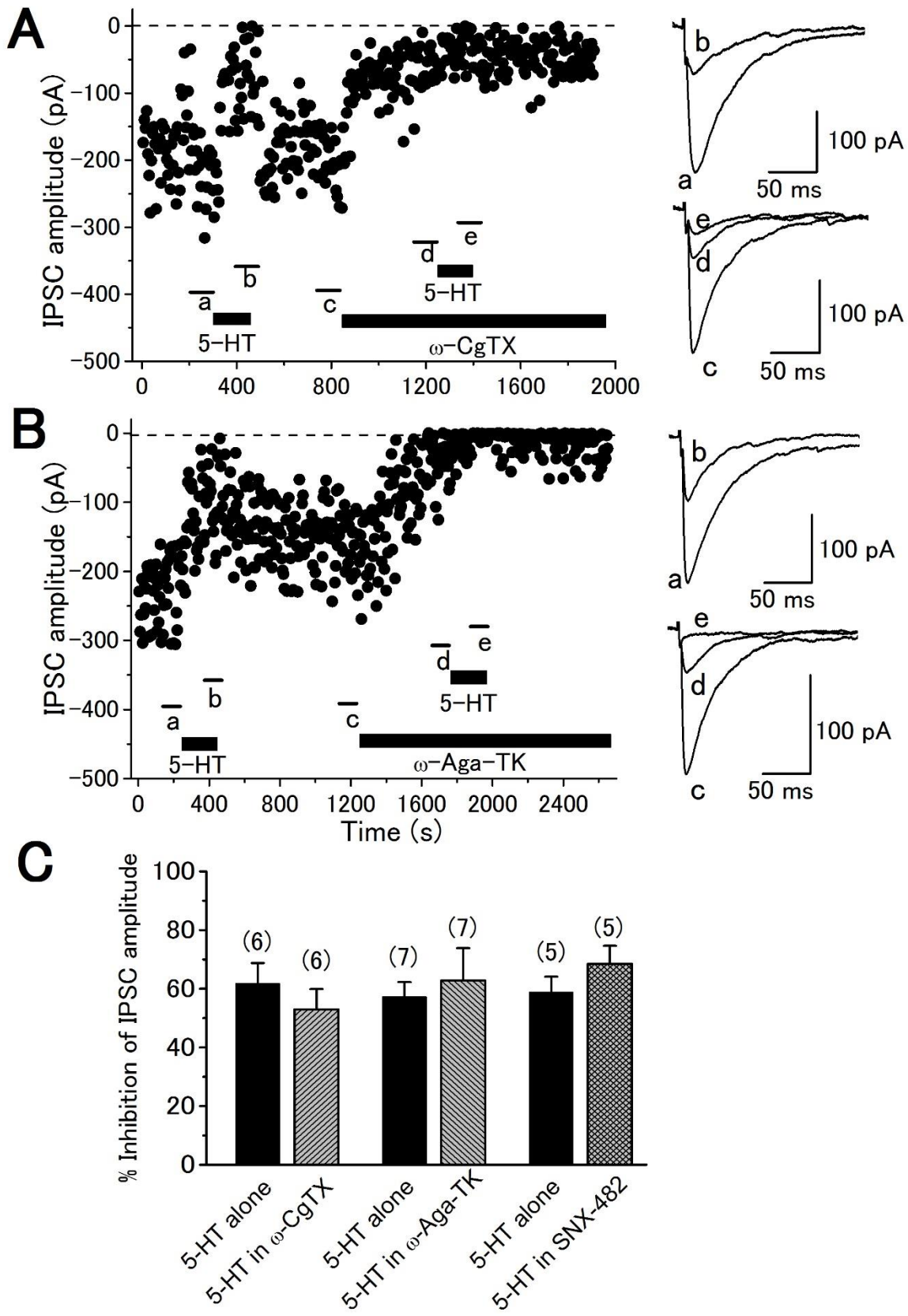


Figure 9

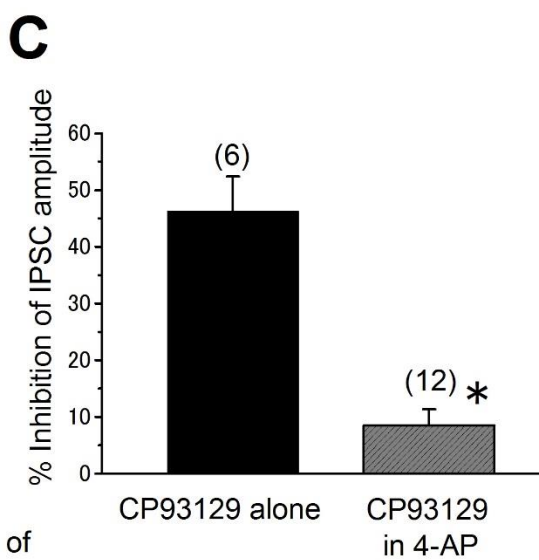
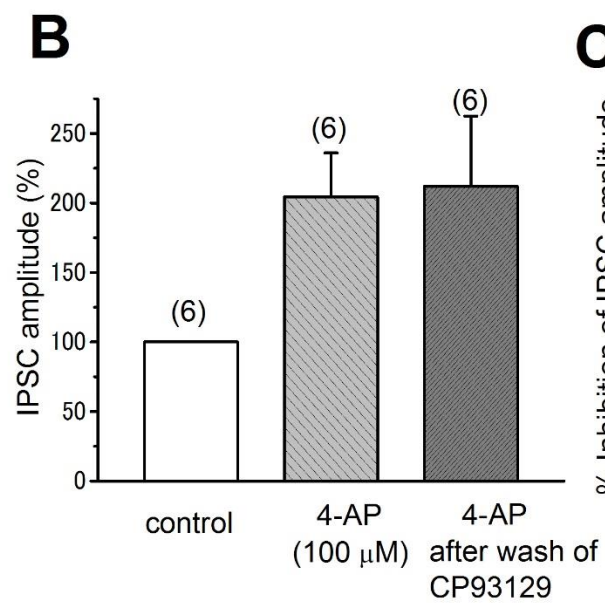
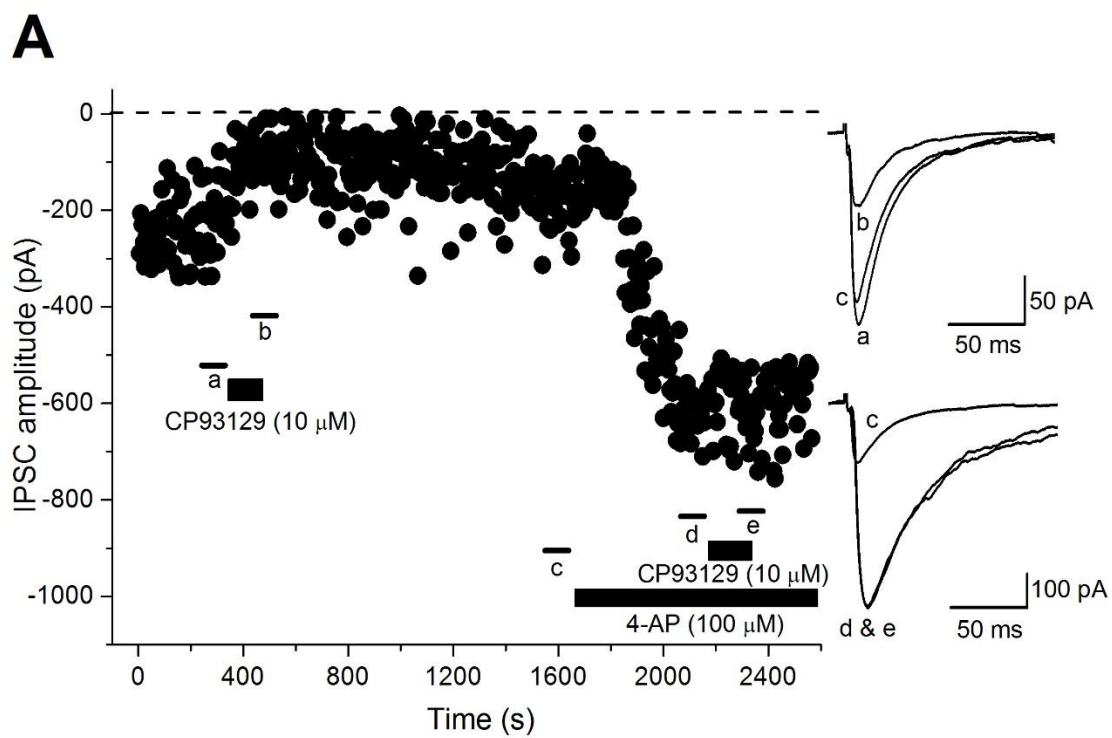
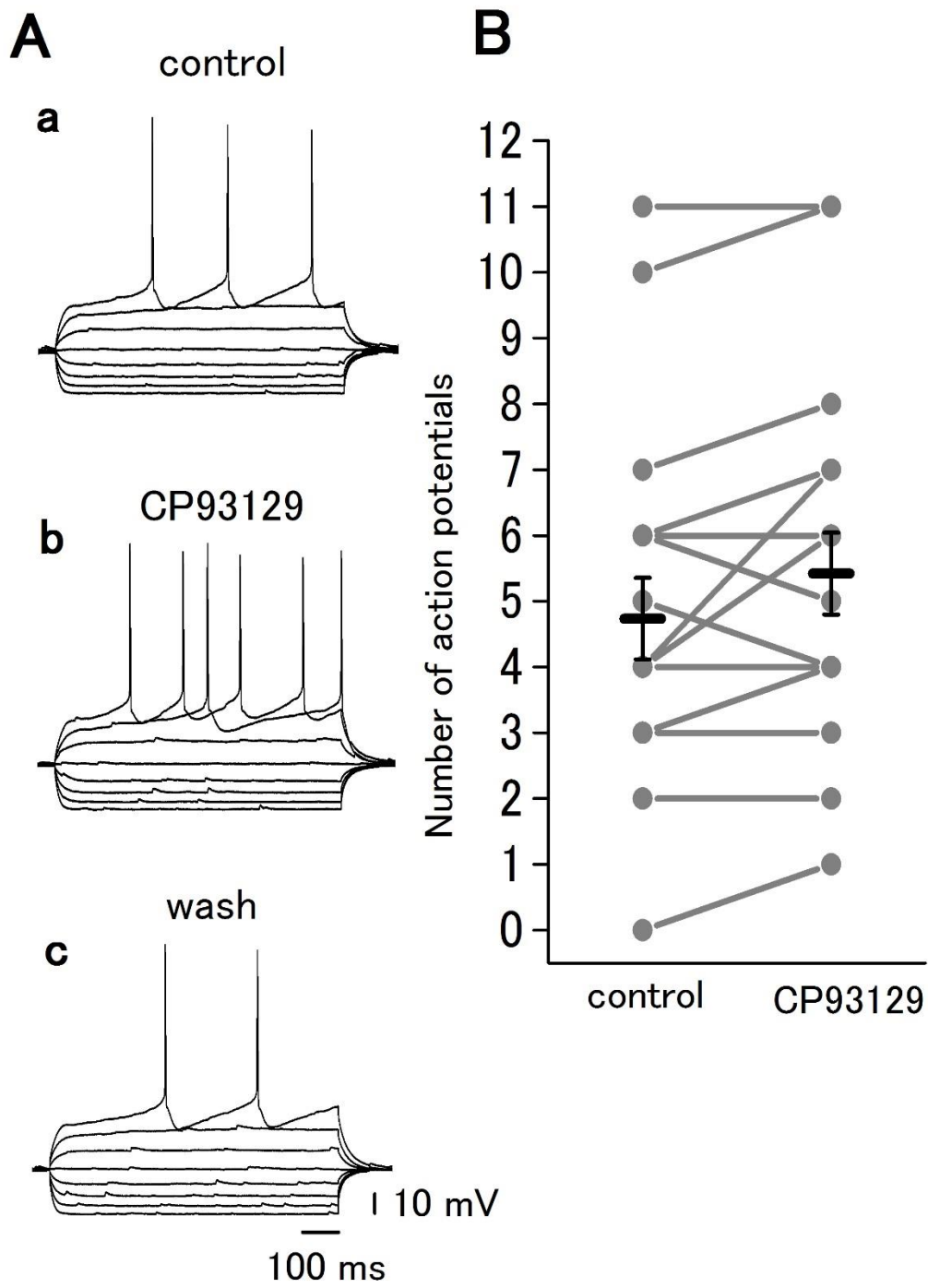


Figure 10



Additional information

Competing interests

The author have no competing interests to declare.

Author contributions

T.M designed the study. T.N and T.M. equally contributed to the experiments, data analyses, interpretation and writing the manuscript.

Funding

This work was supported by The Jikei University Graduate Research Fund, and a Grant-in Aid for Scientific Research from the Ministry of Education, Culture, Sports, Science and Technology of Japan (No. 24500464 to T.M.).

Acknowledgements

The authors are grateful to Drs. T. Ishikawa and J. A. Sim for valuable comments on the data and manuscript. The authors are also grateful to M. Kagata for animal care and technical assistance.